Electronic Supplementary Material (ESI) for Organic Chemistry Frontiers.
This journal is © the Partner Organisations 2016

Electronic Supplementary Information

Supramolecular radical polymers self-assembled from the stacking of radical cations of rod-like viologen di- and trimers

Tian-Guang Zhan,[a,c] Tian-You Zhou,[a] Feng Lin,[a] Liang Zhang,[b] Cen Zhou,[a]
Qiao-Yan Qi,[a] Zhan-Ting Li,[b] and Xin Zhao*[a]

[a] Key Laboratory of Synthetic and Self-Assembly Chemistry for Organic Functional Molecules, Shanghai Institute of Organic Chemistry, Chinese Academy of Sciences, 345 Lingling Road, Shanghai, 200032, China. E-mail: xzhao@mail.sioc.ac.cn

[b] Department of Chemistry, Fudan University, 220 Handan Road, Shanghai 200433, China.

[c] College of Chemistry and Life Science, Zhejiang Normal University, Jinhua 321004, P. R. China.

Table of Contents

Section 1: Materials and General Methods

All reagents were purchased from commercial suppliers and used without further purification unless stated otherwise. Zincke salts **1** and **2** were synthesized according to the literatures[1]. ^1H NMR spectra were recorded on a Bruker Avance DMX 400 spectrometer and ^{13}C NMR spectra were recorded on a 500 MHz Agilent spectrometer at 25°C.

Cyclic Voltammetry: Experiments were performed with a CHI-660D electrochemical working station and saturated calomel electrode (SCE) was used as reference electrode, 0.1 M $^{n-}Bu_4PF_6$ in CH_3CN and 0.1 M KCl in H_2O were used as electrolyte, respectively, and the sample solution was degassed by argon bubbling for two minutes before CV scanning.

UV-Vis and UV-Vis-NIR spectroscopy: absorption spectra for the COV compounds were recorded with a Unico 4802 UV-vis double beam spectrophotometer; and the absorption spectra for the COV radical cations were recorded with a Perlom Elmer Lambda 750S UV-Vis /NIR Spectrophotometer (PerkinElmer, USA).

Fluorescence spectroscopy: spectra were recorded with an F-4600 FL spectrophotometer at 25 °C in CH_3CN and H_2O, respectively.

DFT calculation: Optimized structures and the FMOs of the COVs and their corresponding radical cations were performed with the Gaussian 09 package at the B3LYP/6-31G (d) level without consideration of solvation; the model superstructure for $(MV^{\bullet+})_2\subset CB[8]$ was carried out at the m06/6-31g (d, p) level and the optimized superstructure of $[(PV)^{2\bullet+}]_2\subset CB[8]$ was generated by semi-empirical/upm6 calculation.

Cryo-TEM experiments: samples were prepared by carefully dropping the corresponding solution of an as-prepared radical cation solution onto the carbon coated copper grid, which were quickly frozen in liquid propane, and then submit on a FEI 120kV Tecnai T12 transmission electron microscope for observation;

EPR spectroscopy: samples were prepared by carefully injecting the corresponding solution of an as-prepared radical cation solution into a capillaron, and then submitted to an electron paramagnetic resonance spectrometer.

Section 2: Synthesis and Characterizations

Compound 3: Compound **1** (5.4 g, 15 mmol) and benzene-1,4-diamine (0.54 g, 5 mmol) were dissolved in ethanol (80 mL). The mixture was heated under reflux for 48 h. The hot mixture was filtered and the filtered cake was washed by acetone (2×80 mL). The resulting gray solid was recrystallized from CH_3OH/THF. Compound **3** was obtained as a brown solid (0.15 g, 15%). ^{1}H NMR (400 MHz, CD_3CN): δ (ppm) 9.10 (d, J = 6.8 Hz, 4 H), 8.93 (d, J = 6.0 Hz, 4 H), 8.58 (d, J = 6.4 Hz, 4 H), 8.12 (s, 4 H), 7.92 (d, J = 6.0 Hz, 4 H). ^{13}C NMR (125 MHz, CD_3CN) was obtained from its hexafluorophosphate salt: 152.96, 151.78, 151.76, 151.01, 150.96, 150.04, 150.01, 144.71, 142.86, 140.76, 131.61, 126.66, 125.85, 124.99, 124.39, 123.76, 122.52, 121.91, 121.04, 117.02, 115.06, and 113.53. MS (ESI): *m/2z* 194.1 $[M\text{-}2Cl]^{2+}$. HRMS (MALDI-TOF) Calcd. for $C_{26}H_{20}N_4$ 388.17 $[M\text{-}2PF_6]^+$, Found: $C_{26}H_{19}N_4$ 387.1604 $[M\text{-}2PF_6]^+$.

Compound 4: Compound **1** (3.64 g, 10 mmol) and benzene-1,4-diamine (3.26 g, 30 mmol) were dissolved in anhydrous ethanol (100 mL). The mixture was heated under reflux for 12 h. The hot mixture was filtered and the filtered cake was washed with acetone (300 mL). The resulting brownish red solid was redissolved in a minimum amount of methanol with heating and reprecipitated by the addition of THF. The precipitate was collected and then dried under vacuum to give compound **4** (2.75g, 97%). ^{1}HNMR (400 MHz, DMSO-d_6): δ (ppm) 9.35 (d, J = 7.2 Hz, 2 H), 8.88 (d, J = 6.4 Hz, 2 H), 8.67 (d, J = 6.4 Hz, 2 H), 8.12-8.11 (dd, J_1= 4.4 Hz, J_2= 1.2 Hz, 2 H), 7.56 (d, J = 8.8 Hz, 2 H), 6.68 (d, J = 8.8 Hz, 2 H), 6.00 (s, 2 H). ^{13}CNMR (125 MHz, CD_3CN) was obtained from its hexafluorophosphate salt: 154.22, 152.26, 152.14, 145.05, 142.02, 126.69, 126.07, 122.72, 118.26 and 115.54. MS (ESI): *m/z* 248.0 $[M\text{-}Cl]^+$. HRMS (ESI) Calcd. for $C_{16}H_{14}N_3^+$ [M-Cl]: 248.1185. Found: 248.1182.

Compound 5: A suspension of compound **4** (0.45 g, 0.81mmol) and compound **2** (0.576 g, 2.0 mmol) in anhydrous ethanol (60 mL) were heated under reflux for 84 h. After being cooling down to room temperature, the resulting solid was filtrated and recrystallized from CH_3OH / THF. The gray solid was collected, washed with acetone and dried to offer compound **5** (0.31g, 50%). ^{1}HNMR (400 MHz, D_2O): 9.61 (d, J =

6.4 Hz, 4 H), 9.41 (d, *J* = 6.8 Hz, 4 H), 8.95 (d, *J* = 6.4 Hz, 4 H), 8.89 (d, *J* = 5.2 Hz, 4 H), 8.71 (d, *J* = 6.4 Hz, 4 H), 8.29 (d, *J* =3.6 Hz, 8 H), 8.12 (d, *J* = 5.6 Hz, 4 H). ^{13}CNMR (125 MHz, D_2O): 164.69, 155.63, 151.36, 149.93, 145.86, 144.98, 144.52, 144.12, 144.11, 142.46, 127.52, 126.91, 126.31 and 122.79. MS (ESI): m/3z 206.5 $[M\text{-}4Cl]^{3+}$. HRMS (MALDI-TOF) was obtained from its hexafluorophosphate salt: Calcd. for $C_{42}H_{32}N_6^+$ $[M\text{-}4PF_6]$: 620.2689. Found: 620.2683.

Compound 6: Compound **1** (1.95 g, 5.5 mmol) and benzidine (0.3 g, 1.6 mmol) were dissolved in anhydrous ethanol (120 mL). The mixture was heated under reflux for 12 h. After being cooling down to room temperature, the precipitates were filtrated and washed by another 2×100 mL acetone. Then, the resulting solid was dissolved in 100 mL CH_3OH, to which excess NH_4PF_6 was added and stirred at room temperature for 6h. Compound **6** was obtained by filtrated and dried (0. 905 g, 75%). ^{1}H NMR (400 MHz, DMSO-*d*$_6$): δ (ppm) 9.58 (d, *J* = 6.8 Hz, 4 H), 8.93 (d, *J* = 6.0 Hz, 4 H), 8.84 (d, *J* = 6.8 Hz, 4 H), 8.25 (d, *J* = 8.8 Hz, 4 H), 8.18 (d, *J* = 4.2 Hz, 4 H), 8.12 (d, *J* = 8.4 Hz, 4 H). ^{13}C NMR (125 MHz, DMSO-*d*$_6$): 153.42, 152.05, 150.29, 146.45, 145.53, 145.23, 144.35, 142.28, 140.87, 140.63, 129.92, 128.83, 128.63, 127.52, 126.91, 126.19, 125.76, 125.49, 124.51, 123.31, 122.21, and 120.94. MS (ESI): *m/2z* 232.1 $[M\text{-}2Cl]^{2+}$. HRMS (MALDI-TOF) Calcd. for $C_{32}H_{24}N_4$ 464.20 $[M\text{-}2PF_6]^+$, Found: $C_{32}H_{23}N_4$ 463.1917 $[M\text{-}2PF_6]^+$.

Compound 7: Compound **1** (3.62 g, 10 mmol) and benzidine (7.61 g, 40 mmol) were dissolved in anhydrous ethanol (350 mL). The mixture was heated under reflux for 12 h. The red precipitates were filtrated by hot and washed by another 3×100mL acetone, the resulting solid was filtrated and recrystallized from CH_3OH / THF. Compound **7** was obtained as a red solid (2.82 g, 80%). ^{1}H NMR (400 MHz, CD_3CN): δ (ppm) 9.07 (d, *J* = 6.8 Hz, 2 H), 8.87 (d, *J* = 6.0 Hz, 2 H), 8.48 (d, *J* = 6.8 Hz, 2 H), 7.90 (t, *J* = 8.8 Hz, 2 H), 7.74 (d, *J* = 8.8 Hz, 4 H), 7.53 (d, *J* = 8.8 Hz, 2 H), 6.77 (d, *J* = 8.8 Hz, 2 H). ^{13}CNMR (125 MHz, CD_3CN) was obtained from its hexafluorophosphate salt: 152.83, 151.09, 149.59, 144.99, 143.48, 140.61, 139.72, 127.72, 126.36, 125.25, 124.95, 124.80, 122.00, 121.89, and 114.24. MS (ESI): *m/z* 324.1 $[M\text{-}Cl]^+$. HRMS (ESI) Calcd. for $C_{22}H_{18}N_3$ 324.15 $[M\text{-}Cl]^+$, Found: $C_{22}H_{18}N_3$

324.14952 [M-Cl]$^+$.

Compound 8: Compound **2** (0.28 g, 0.5 mmol) and Compound **7** (0.41 g, 1.14 mmol) were dissolved in anhydrous ethanol (50 mL). The mixture was heated under reflux for 72 h. The precipitates were filtrated and washed by another 100 mL acetone, the resulting solid was filtrated and recrystallized from CH_3OH / THF. Compound **8**was obtained as a yellowish green solid (0.34 g, 90%). ^{1}HNMR (400 MHz, CD_3OD): δ (ppm) 9.70 (d, J = 6.4 Hz, 4 H), 9.49 (d, J = 6.8 Hz, 4 H), 9.02 (d, J = 6.4 Hz, 4 H), 8.95 (d, J = 5.6 Hz, 4 H), 8.77 (d, J = 6.8 Hz, 4 H), 8.26 (t, J = 8.0 Hz, 8 H), 8.17 (d, J = 6.8 Hz, 8 H), 8.11 (d, J = 8.4 Hz, 4 H). ^{13}CNMR (125 MHz, DMSO-d_6) was obtained from its hexafluorophosphate salt: 153.43, 151.17, 149.07, 145.95, 145.39, 142.30, 140.60, 128.72, 126.68, 125.68, 125.32, and 122.09. MS (ESI): *m/3z* 257.4 [M-4Cl]$^{3+}$. HRMS (MALDI-TOF) Calcd. for $C_{54}H_{40}N_6$ 772.33 [M-4PF$_6$]$^+$, Found: $C_{54}H_{40}N_6$ 772.3309 [M-4PF$_6$]$^+$.

Compound PV2: 0.233g (0.5mmol) compound **3**, 1 mL CH_3I and 60 mL anhydrous CH_3CN were added in a sealed tube, which was heated to reflux for 12h. after cooling to room temperature, the precipitates were filtrated and washed with 3×50 mL acetone. The resulting red solid was collected and dissolved in 10 mL H_2O, and 0.6 g NH_4PF_6 was added. The suspension was stirred for another 6 h, precipitates were filtrated and dried. **PV2(4PF$_6$)** was obtained as brown solid (0.34 g, 70%). ^{1}H NMR (400 MHz, CD_3CN): δ (ppm) 9.28 (d, J = 6.8 Hz, 4 H), 8.95 (d, J = 6.4 Hz, 4 H), 8.67 (d, J = 6.8 Hz, 4 H), 8.51 (d, J = 6.0 Hz, 4 H), 8.18 (s, 4 H), 4.46 (s, 6 H). ^{13}C NMR (125 MHz, CD_3CN): 152.47, 149.95, 147.44, 146.81, 145.22, 128.51, 128.25, 128.00, 127.96, 127.82, and 49.45. HRMS (MALDI-TOF) Calcd. for $C_{28}H_{26}N_4$ 418.21 [M-4PF$_6$]$^+$, Found: $C_{28}H_{26}N_4$ 418.2152 [M-4PF$_6$]$^+$.

Compound PV3: The synthesis presedure was similar to **PV2**, and Compound **PV3(6PF$_6$)** was obtained as dark brown solid in a yield of 80%. ^{1}H NMR (400 MHz, CD_3CN): δ (ppm) 9.34 (d, J = 6.4 Hz, 4 H), 9.29 (d, J = 6.4 Hz, 4 H), 8.96 (d, J = 7.2 Hz, 4 H), 8.79 (d, J = 6.4 Hz, 4 H), 8.68 (d, J = 6.8 Hz, 4 H), 8.52 (d, J = 6.4 Hz, 4 H), 8.21 (s, 8 H), 4.46 (s, 6 H). ^{13}C NMR (125 MHz, CD_3CN): 151.73, 151.24, 149.18, 146.66, 146.04, 145.88, 144.52, 127.77, 127.51, 127.26, 127.08, and 48.73. HRMS

(MALDI-TOF) Calcd. for $C_{44}H_{38}N_6$ 650.3158 [M-6PF$_6$]$^+$, Found: $C_{44}H_{38}N_6$ 650.3153 [M-6PF$_6$]$^+$.

Compound BPV2: The synthesis presedure was similar to **PV2**, and Compound **BPV2(4PF$_6$)** was obtained as earthy yellow solid in a yield of 90%. ^{1}H NMR (400 MHz, CD_3CN): δ (ppm) 9.26 (d, J = 6.4 Hz, 4 H), 8.94 (d, J = 6.0 Hz, 4 H), 8.63 (d, J = 6.4 Hz, 4 H), 8.50 (d, J = 6.0 Hz, 4 H), 8.16 (d, J = 8.0 Hz, 4 H), 7.97 (d, J = 8.4 Hz, 4 H), 4.48 (s, 6 H). ^{13}C NMR (125 MHz, CD_3CN): 150.86, 149.32, 146.62, 145.56, 142.39, 142.15, 129.52, 127.29, 126.97, 125.31, and 48.65. HRMS (MALDI-TOF) Calcd. for $C_{34}H_{30}N_4$ 494.24 [M-4PF$_6$]$^+$, Found: $C_{34}H_{30}N_4$ 494.2465 [M-4PF$_6$]$^+$.

Compound BPV3: The synthesis presedure was similar to Compound **PV2**, and **BPV3(6PF$_6$)** was obtained as brown solid in a yield of 90%. ^{1}H NMR (400MHz, CD_3CN): δ (ppm) 9.30 (d, J = 6.4 Hz, 4 H), 9.25 (d, J = 6.4 Hz, 4 H), 8.91 (d, J = 6.4 Hz, 4 H), 8.74 (d, J = 6.0 Hz, 4 H), 8.63 (d, J = 6.4 Hz, 4 H), 8.49 (d, J = 6.4 Hz, 4 H), 8.18 (t, J = 8.4 Hz, 8 H), 7.99 (t, J = 18.4 Hz, 8 H), 4.45 (s, 6 H). ^{13}C NMR (100MHz, CD_3CN): 150.89, 150.56, 149.33, 146.61, 145.69, 145.58, 142.43, 142.40, 142.24, 142.19, 129.58, 129.56, 127.49, 127.31, 127.01, 125.36, 125.33, and 48.69. HRMS (MALDI-TOF) Calcd. for $C_{56}H_{46}N_6$ 802.38 [M-6PF$_6$]$^+$, Found: $C_{56}H_{46}N_6$ 802.3770 [M-6PF$_6$]$^+$.

The chloride salts of the COVs were prepared by anion exchange of their hexafluorophosphate (PF$_6$) salts with TBACl. A typical procedure is described as follows. The PF$_6$ salt of a COV was dissolved in a minimum amount of CH_3NO_2. Excess tetrabutylammonium chloride (TBACl) was added and the resulting suspension was then stirred at room temperature for 2 hours. The precipitate was collected and washed by acetone and dried under vacuum to afforded chloride salt of the COV as a brown solid.

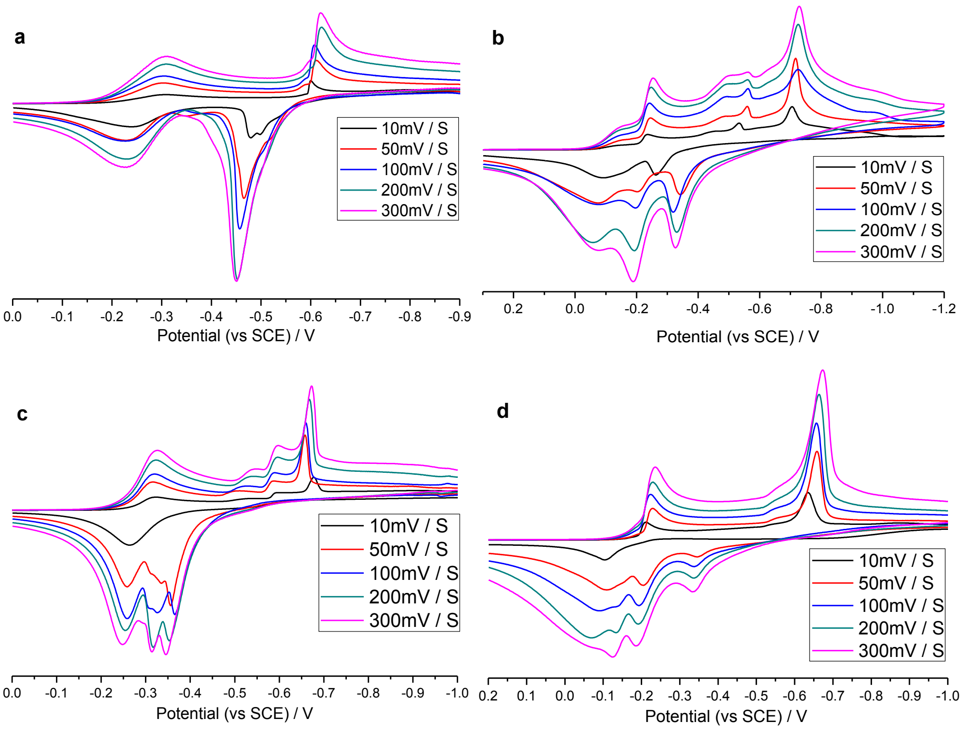

Figure S1. Cyclic voltammograms (vs SCE) of (a) **PV2**, (b) **PV3**, (c) **BPV2**, and (d) **BPV3** recorded at a variety of scan rate from 0.01 V/S to 0.3 V/S in CH_3CN at 25 ^{o}C. The concentrations of the COV samples and electrolyte were 1.0 mM and 0.1 M, respectively.

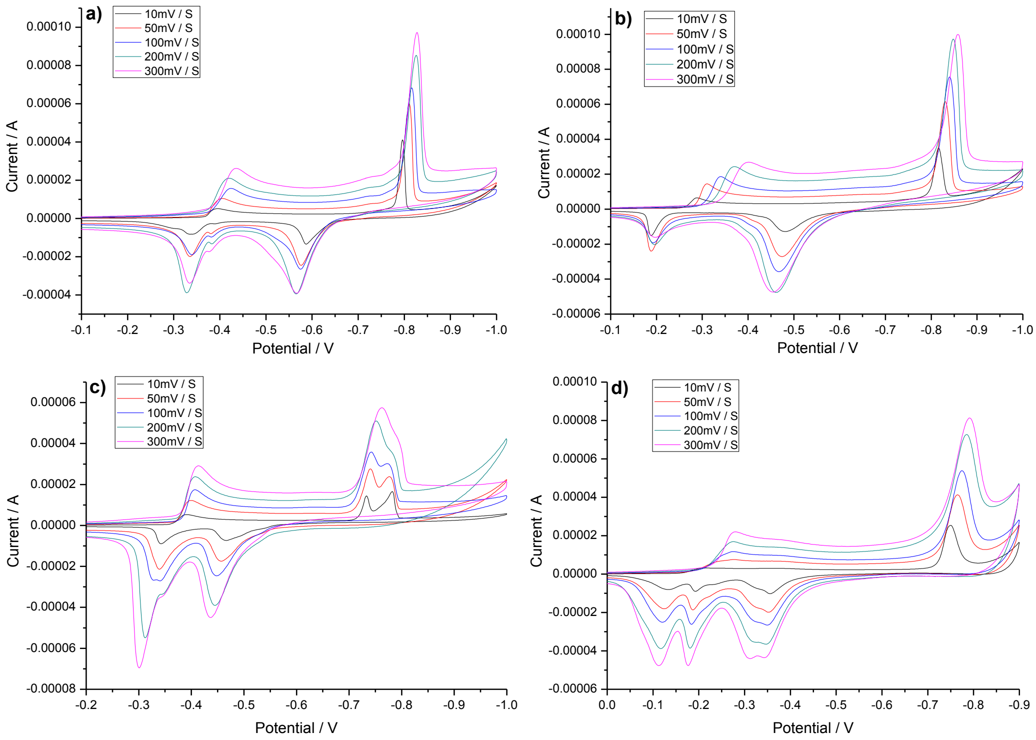

Figure S2. Cyclic voltammograms (vs SCE) of (a) **PV**2, (b) **PV3**, (c) **BPV2** and (d) **BPV3** in H_2O recorded at a variety of scan rate from 0.01 V/S to 0.3V/S at 25 ^{o}C. The concentrations of the COV samples and electrolyte were 1.0 mM and 0.1 M, respectively.

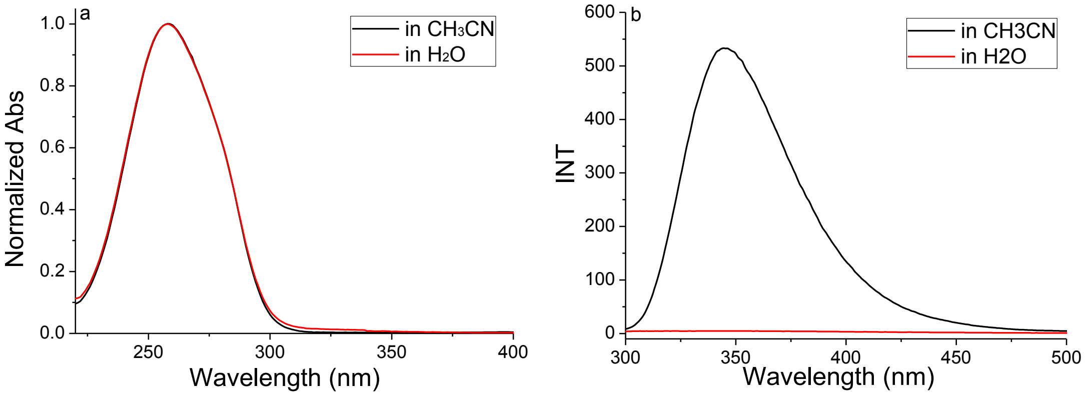

Figure S3. (a) Normalized Uv-vis spectra of **MV** (0.01 mM) in CH_3CN and H_2O at 25 °C, respectively. (b) Fluorescence spectra of **MV** (0.01 mM) (λ_{ex} = 260 nm) in CH_3CN and H_2O at 25 °C, respectively.

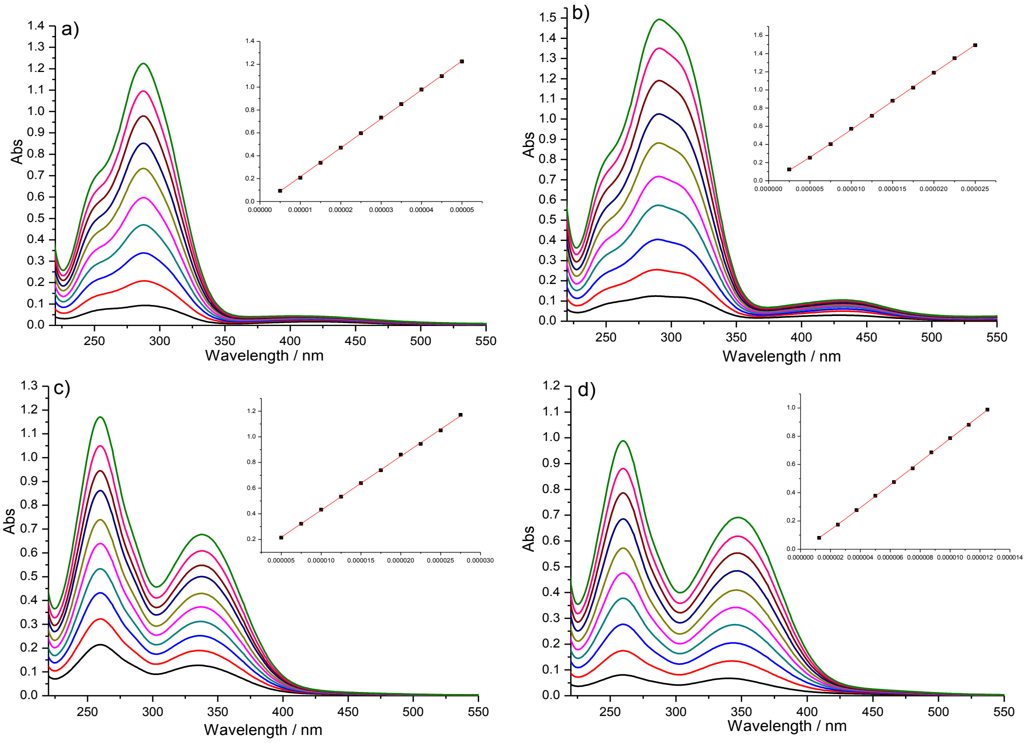

Figure S4. UV-vis dilution spectra of (a) **PV2** (0.005 to 0.05 mM), (b) **PV3** (0.0025 to 0.025 mM), (c) **BPV2** (0.005 to 0.0275 mM) and (d) **BPV3** (0.00125 to 0.0125 mM) in CH_3CN at 20 ^oC. Inset: absorbance at λ_{max} vs concentration plot.

í

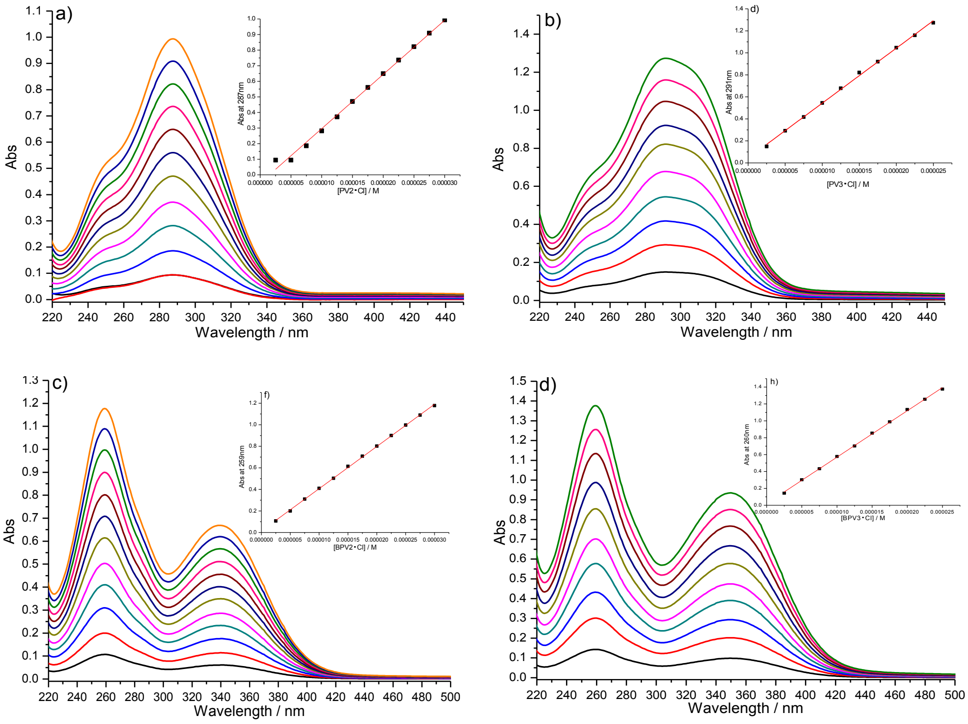

Figure S5. UV-vis absorption spectra of (a) **PV2** (0.0025 to 0.03 mM), (b) **PV3** (0.0025 to 0.025 mM), (c) **BPV2** (0.0025 to 0.03 mM) and (d) **BPV3** (0.0025 to 0.025 mM) in H_2O at 20 °C. Inset: absorbance at λ_{max} vs concentration plot.

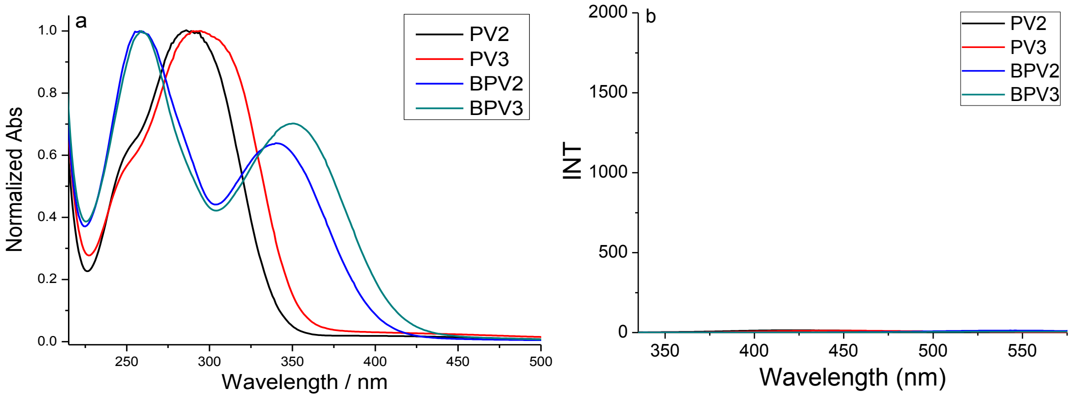

Figure S6. (a) Normalized Uv-vis absorption spectra of **PV2**, **PV3**, **BPV2** and **BPV3** in H_2O at 20 °C and (b) Fluorescence spectra of **PV2**, **PV3**, **BPV2** and **BPV3** (λ_{ex} = 290 nm) at 25 °C in H_2O. The concentration was 5.0×10^{-6} M.

Table S1 Summary of Optical and Electrochemical Properties of the COVs in CH_3CN and (H_2O).

Compounds	λ_{max}^{abs}/nm	λ_{max}^{em}/nm	$\varepsilon \times 10^4$/$M^{-1}cm^{-1}$	$E_{1/2}^{red-1}$/V
MV	260 (258)	345 (/)	2.08 (2.53)	-0.42 (-0.66)
PV2	287 (289)	436 (/)	3.50 (3.48)	-0.23 (-0.39)
PV3	292 (294)	454 (/)	4.17 (5.00)	-0.21 (-0.32)
BPV2	348 (349)	550 (/)	5.60 (3.92)	-0.28 (-0.39)
BPV3	348 (351)	560 (/)	8.16 (5.50)	-0.14 (-0.18)

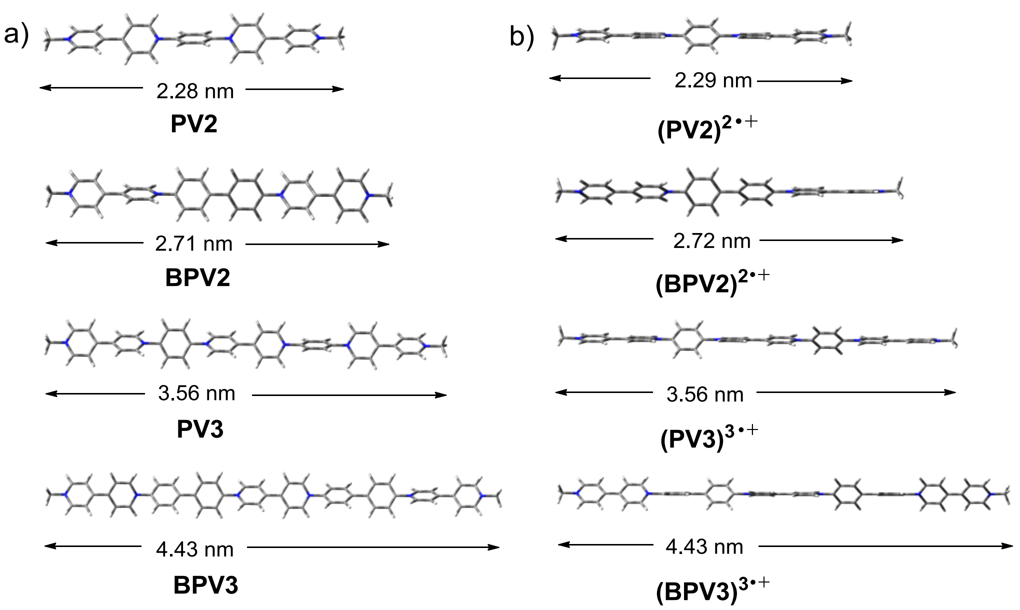

Figure S7. Optimized structures of (a) **PV2** , **PV3, BPV2** and **BPV3**, and (b) (**PV2**)$^{2\ \cdot+}$, (**PV3**)$^{3\ \cdot+}$, (**BPV2**)$^{2\ \cdot+}$ and (**BPV3**)$^{3\ \cdot+}$ by DFT calculations at B3LYP/6-31G(d) level.

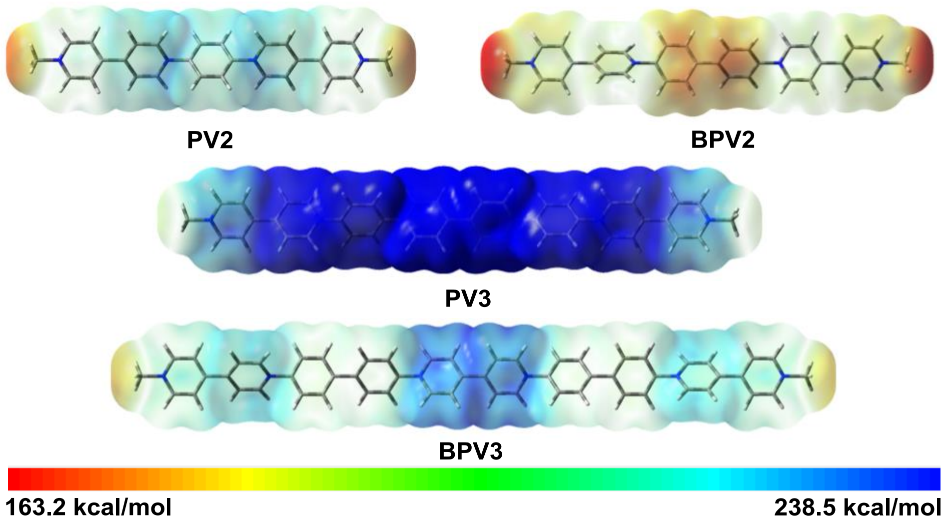

Figure S8. The electron spin polarization (ESP) map [kcal mol^{-1}] of the conjugated oligomeric viologens.

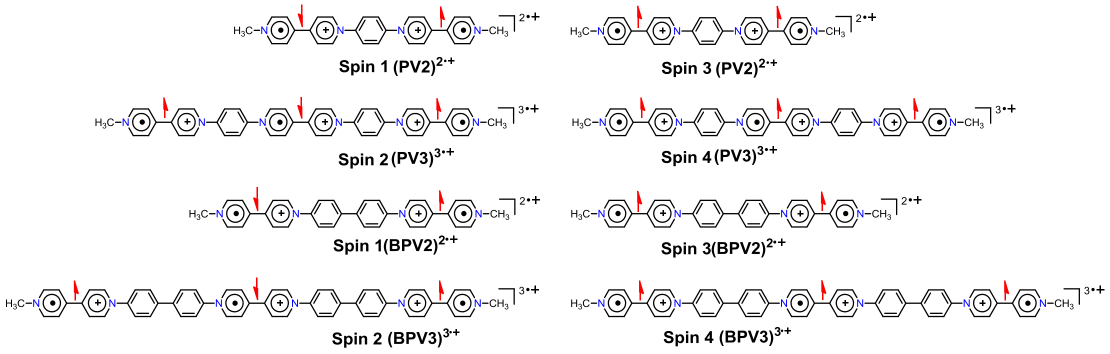

Figure S9. Spin states of the COV radical cations.

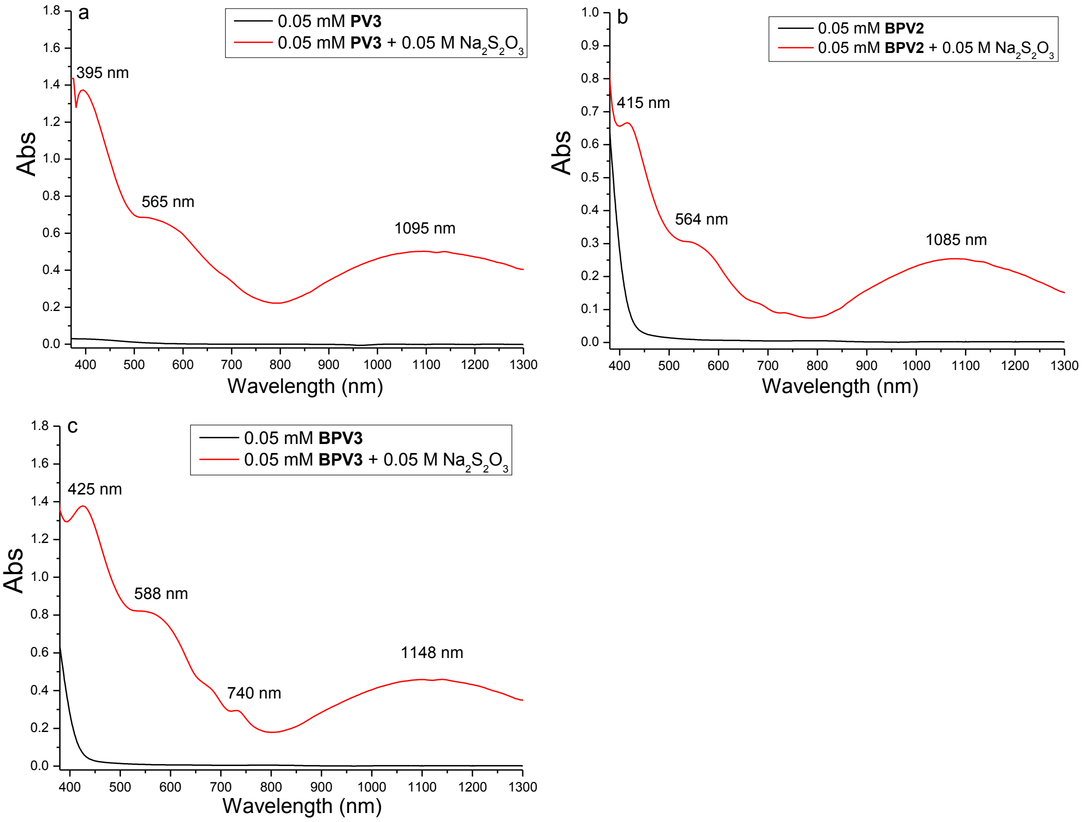

Figure S10. UV-vis-NIR spectra of (a) **PV**3, (b) **BPV2** and (c) **BPV3** before and after reduced by 0.05 M $Na_2S_2O_3$ in H_2O (pH = 7) at 20 ^oC.

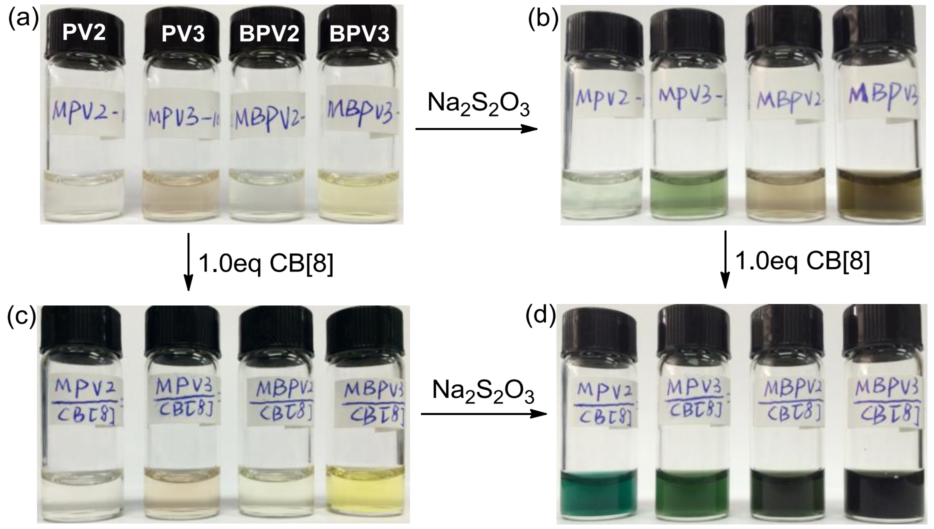

Figure S11. Solution color pictures of **PV2**, **PV3**, **BPV2** and **BPV3** (a) in H_2O; (b) reduced by excess $Na_2S_2O_3$; (c) with 1.0 eq CB[8] in H_2O and (d) solution (c) reduced by excess $Na_2S_2O_3$. The concentration was 0.1 mM at 20 ^oC.

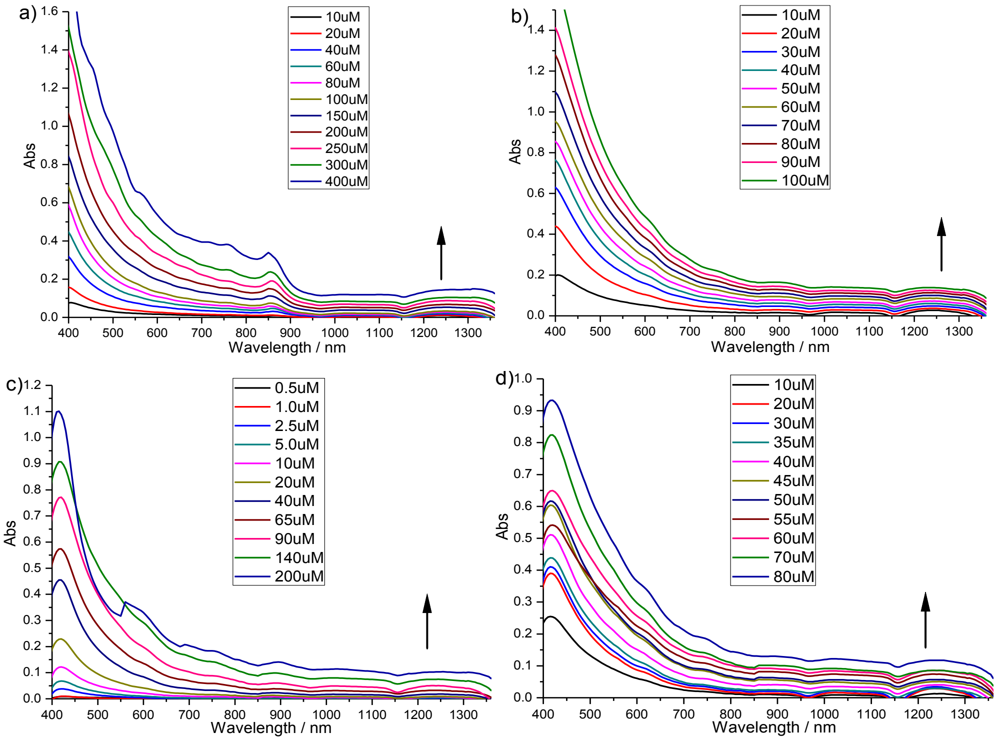

Figure S12. UV-vis-NIR titration spectra of (a) **PV2**, (b) **PV3**, (c) **BPV2** and (d) **BPV3** after being reduced by sodium hydrosulfite (0.05 M) at 60 °C in water (pH = 7).

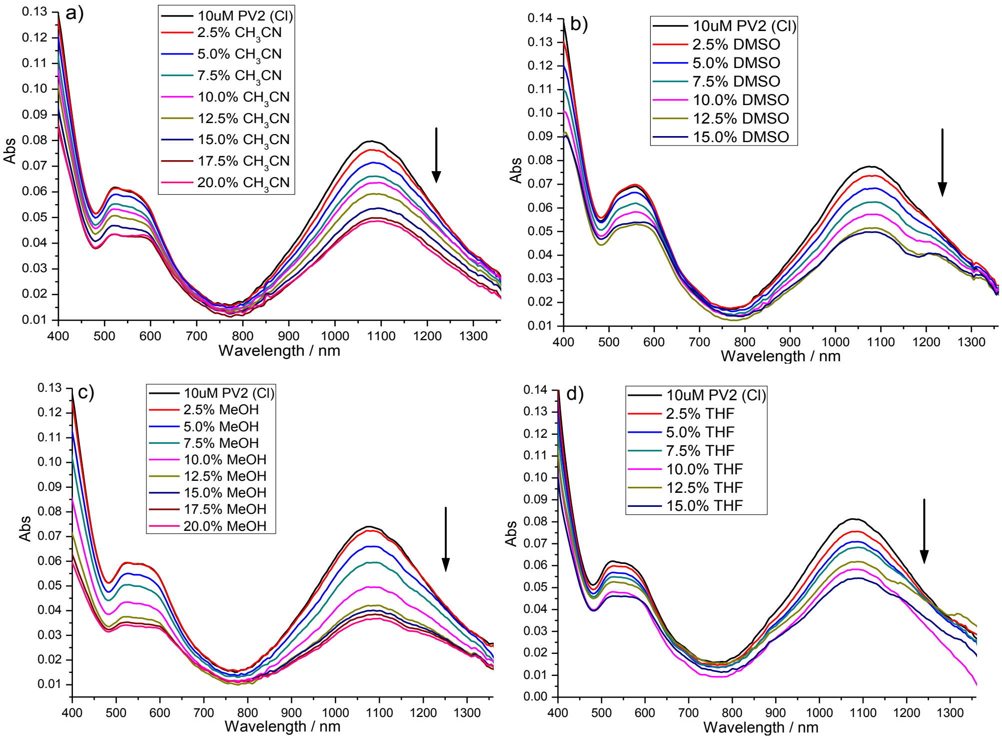

Figure S13. UV-vis-NIR spectra of **PV2** in water with different amount of organic solvents at a concentration of 1×10^{-5} M, a) CH_3CN, b) DMSO, c) MeOH and d) THF (pH = 7) after being reduced by sodium hydrosulfite (0.05 M) at 20 °C.

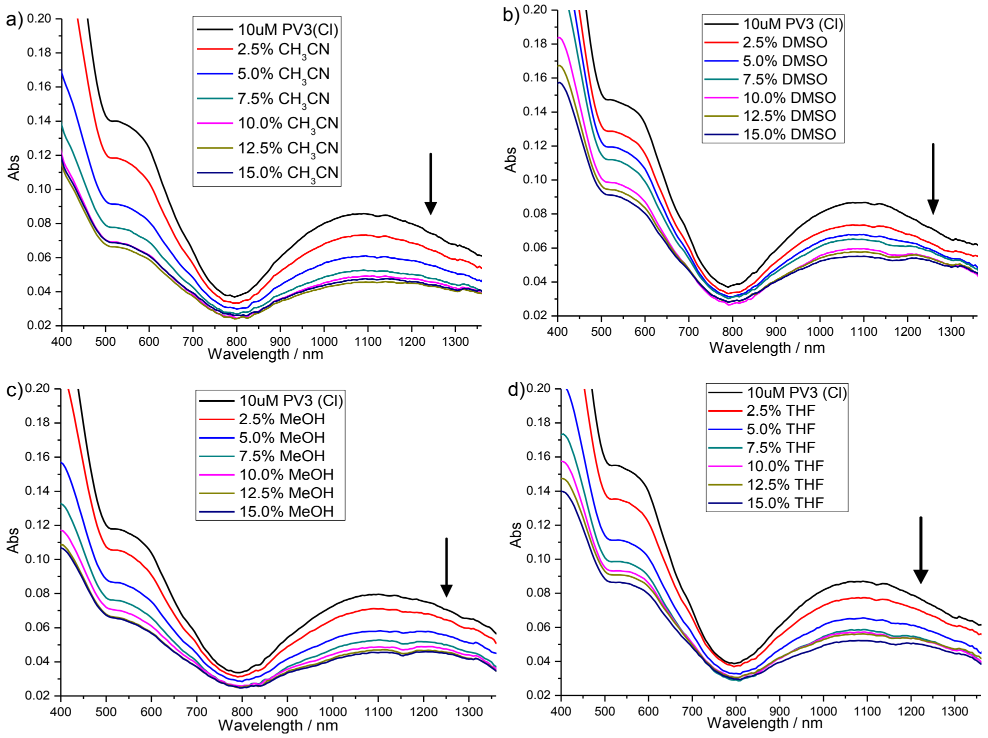

Figure S14. UV-vis-NIR spectra of **PV3** in water with different amount of organic solvents at a concentration of 1×10^{-5} M, a) CH_3CN, b) DMSO, c) MeOH and d) THF (pH = 7) after being reduced by sodium hydrosulfite (0.05 M) at 20 °C.

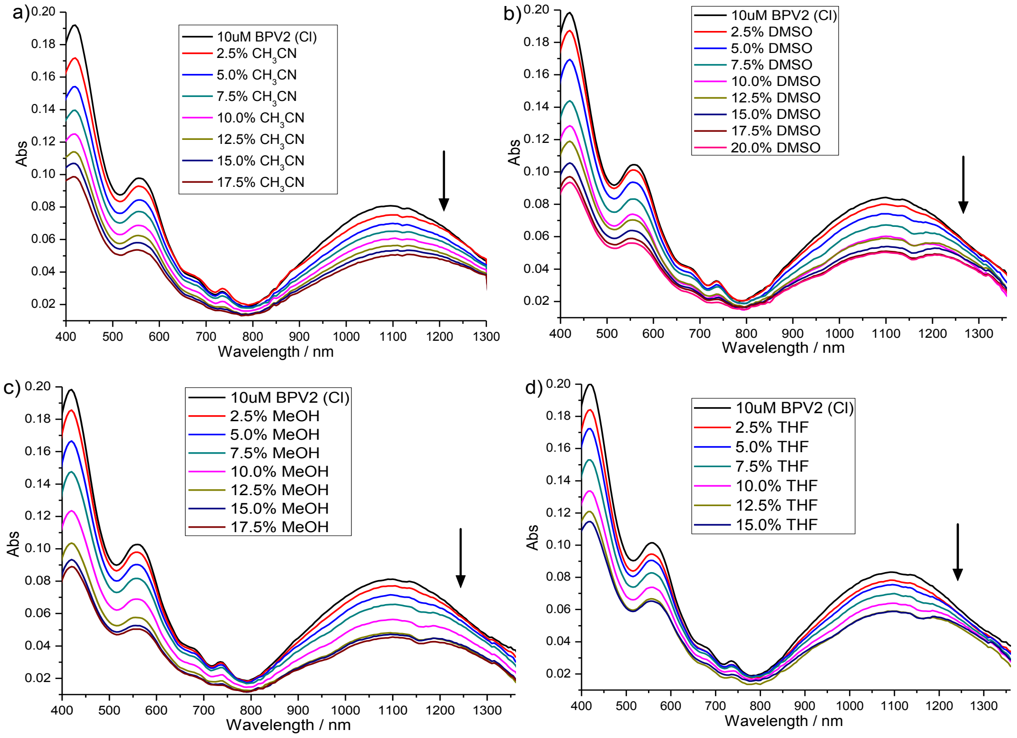

Figure S15. UV-vis-NIR spectra of **BPV2** in water with different amount of organic solvents at a concentration of 1×10^{-5} M, a) CH_3CN, b) DMSO, c) MeOH and d) THF (pH = 7) after reduced by sodium hydrosulfite (0.05 M) at 20 °C.

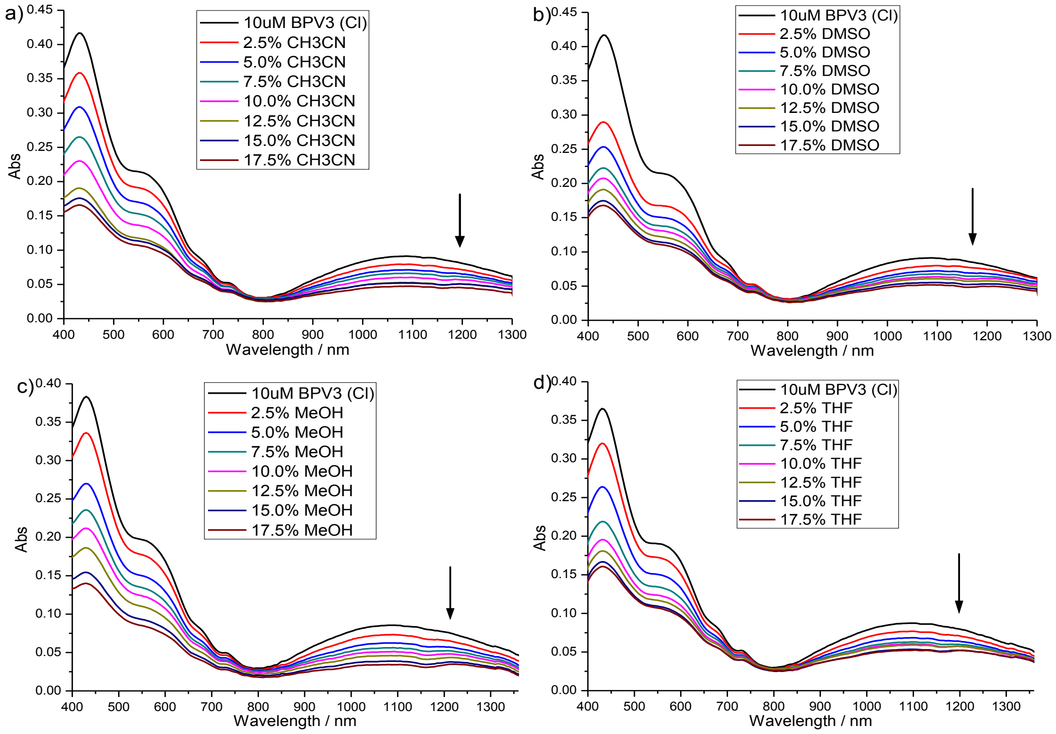

Figure S16. UV-vis-NIR spectra of BPV3 in water with different amount of organic solvents at a concentration of 1×10^{-5} M, a) CH_3CN, b) DMSO, c) MeOH and d) THF (pH = 7) after reduced by sodium hydrosulfite (0.05 M) at 20 ^{o}C.

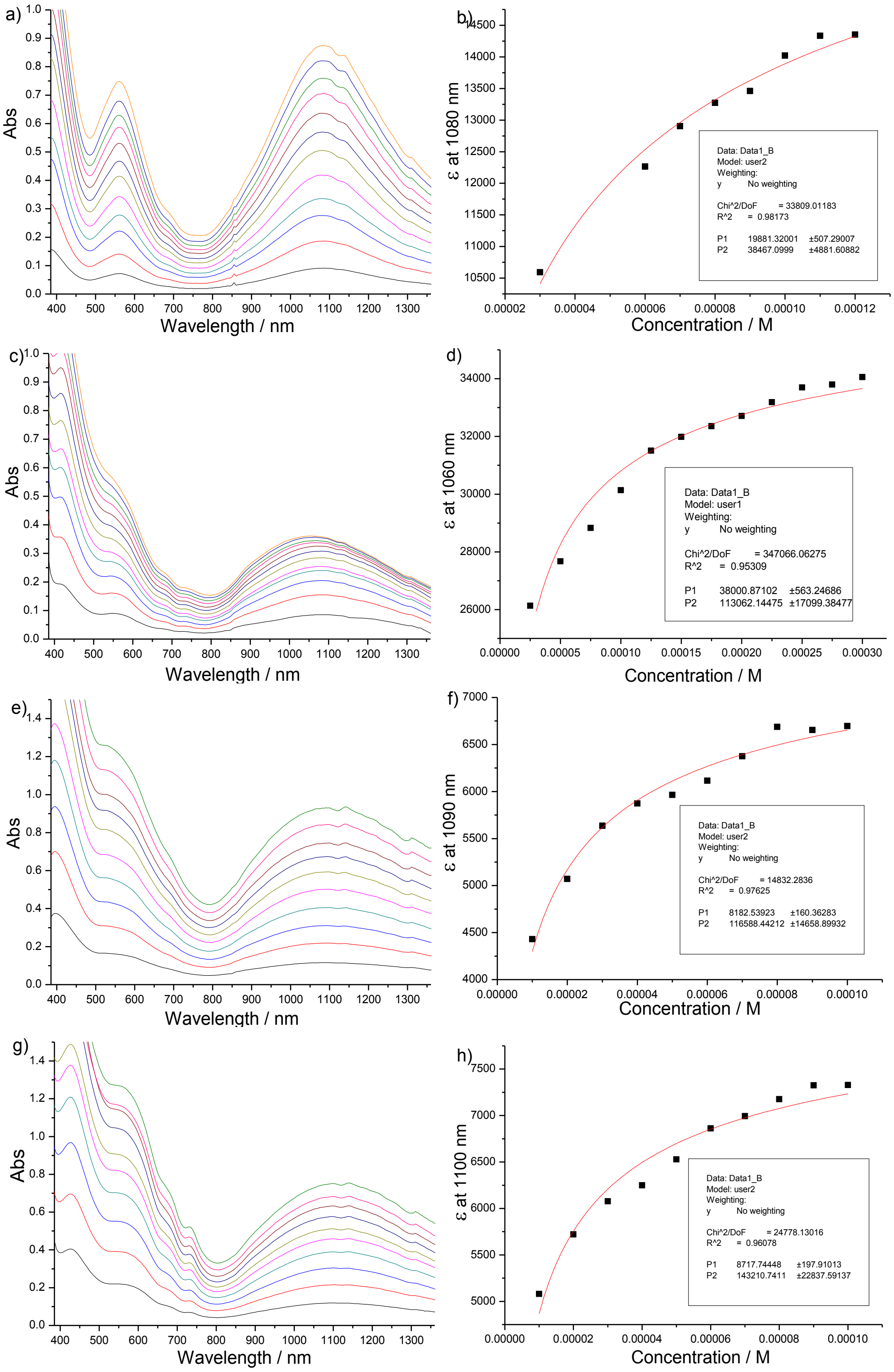

Figure S17. a) UV-vis-NIR dilution spectra of (**PV2**)$^{2\bullet+}$ (0 to 0.12 mM) and b) molar absorption coefficient plot of (**PV2**)$^{2\bullet+}$ at 1080 nm; c) UV dilution spectra of (**BPV2**)$^{2\bullet+}$ (0 to 0.30 mM) and d) molar absorption coefficient plot of (**BPV2**)$^{2\bullet+}$ at 1060 nm; e) UV dilution spectra of (**PV3**)$^{3\bullet+}$ (0 to 0.10 mM) and f) molar absorption coefficient plot of (**PV3**)$^{3\bullet+}$ at 1090 nm; g) UV dilution spectra of (**BPV3**)$^{3\bullet+}$ (0 to 0.10 mM) and h) molar absorption coefficient plot of (**BPV3**)$^{3\bullet+}$ at 1100 nm.

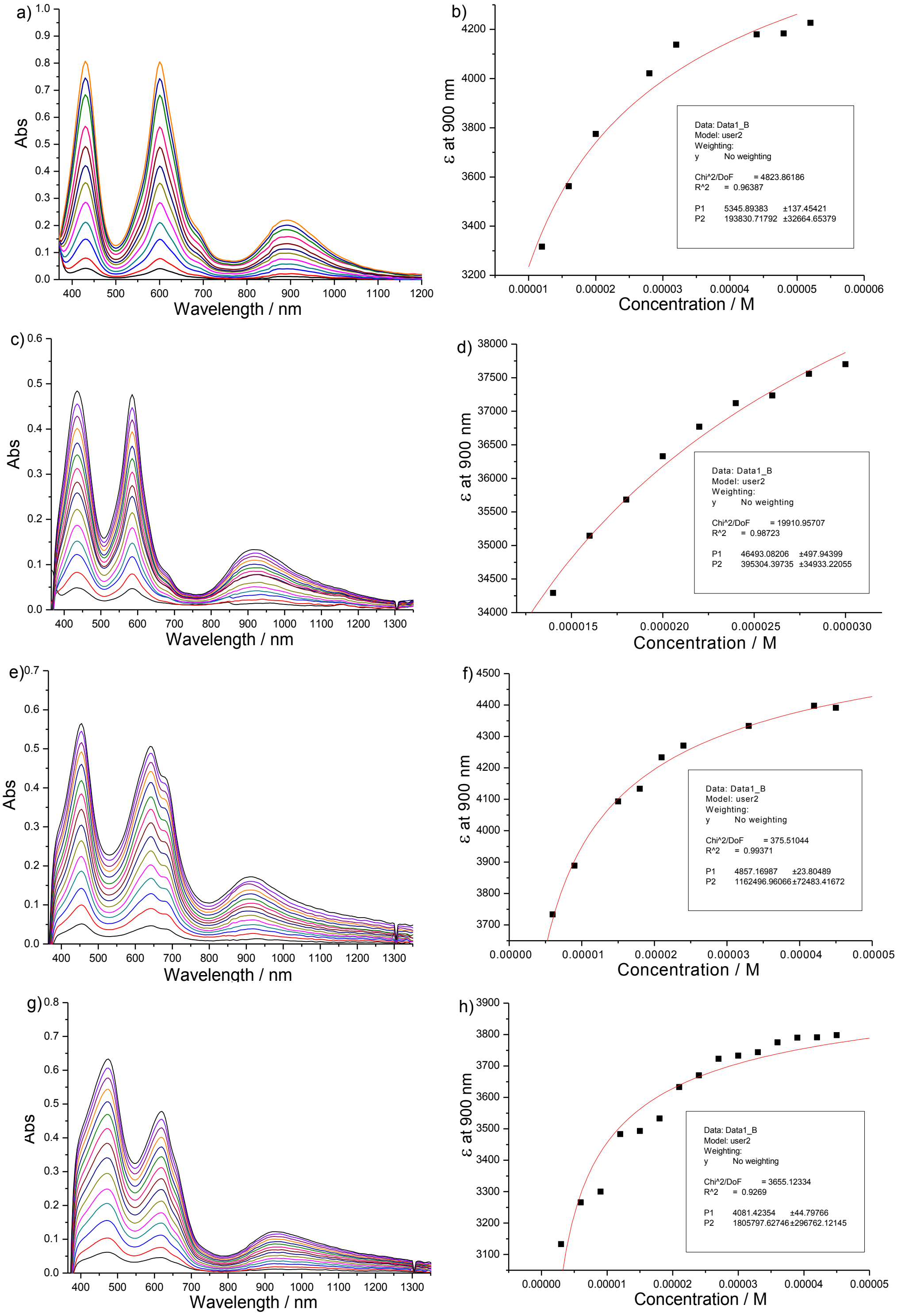

Figure S18. a) UV-vis-NIR dilution spectra of (**PV2**)$^{2\bullet+}$ with 1.0 equiv. CB[8] (0 to 0.026 mM) and b) Molar absorption coefficient plot of (**PV2**)$^{2\bullet+}$ with 1.0 equiv. CB[8] at 900 nm; c) UV dilution spectra of (**BPV2**)$^{2\bullet+}$ (0 to 0.015 mM) and d) molar absorption coefficient plot of (**BPV2**)$^{2\bullet+}$ with 1.0 equiv. CB[8] at 900 nm; e) UV dilution spectra of (**PV3**)$^{3\bullet+}$ (0 to 0.015 mM) and f) molar absorption coefficient plot of (**PV3**)$^{3\bullet+}$ with 1.0 equiv. CB[8] at 900 nm; g) UV dilution spectra of (**BPV3**)$^{3\bullet+}$ (0 to 0.015 mM) and h) molar absorption coefficient plot of (**BPV3**)$^{3\bullet+}$ with 1.0 equiv. CB[8] at 900 nm.

Table S2 Summary of the apparent binding constants (K_a) of the radical cations [a]

Compound	$(MV)^{\cdot+}$	$(PV2)^{2\cdot+}$	$(BPV2)^{2\cdot+}$	$(PV3)^{3\cdot+}$	$(BPV3)^{3\cdot+}$
without CB[8]	$(3.80\sim8.40) \times 10^2$	$(3.85 \pm 0.48) \times 10^4$	$(1.13 \pm 0.17) \times 10^5$	$(1.17 \pm 0.15) \times 10^5$	$(1.43 \pm 0.23) \times 10^5$
with 1.0 eq CB[8]	(2.0×10^7)[b]	$(1.94 \pm 0.33) \times 10^5$	$(3.95 \pm 0.35) \times 10^5$	$(1.16 \pm 0.072) \times 10^6$	$(1.81 \pm 0.29) \times 10^6$

[a] in sodium phosphate buffer (pH = 7.0) of aqueous binary media with the presence of excess sodium dithionite (0.05M), ref2.

[b] dimerization constants for $(MV^{\cdot+})_2 \subset CB[8]$, ref3.

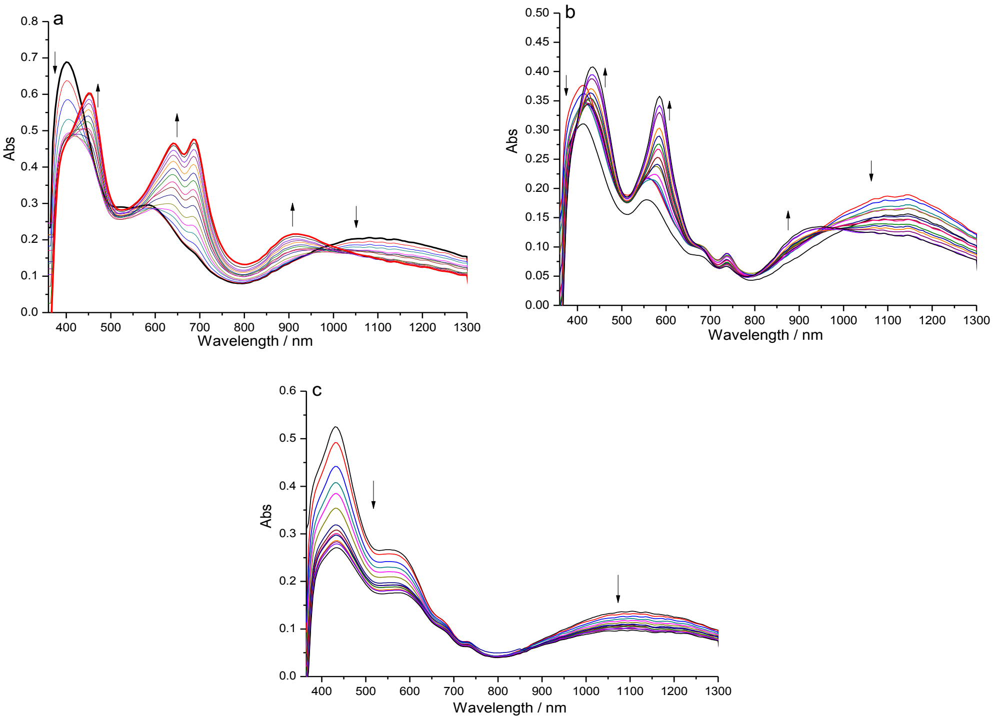

Figure S19. Uv-vis-NIR titration spectra of (a) **PV3**, (b) **BPV2** and (c) **BPV3** with CB[8] (from 0.1 to 1.5 eq) at 20 °C in the presence of 0.05 M sodium hydrosulfite. The concentration of conjugated radical cation was 2.5×10^{-5} M in H_2O.

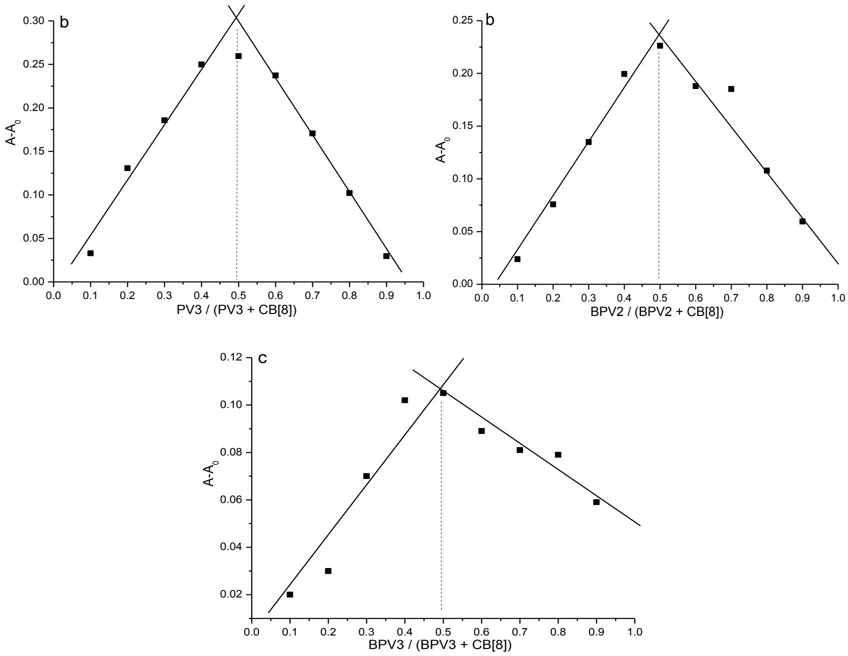

Figure S20. Job's plots of (a) **PV3**, (b) **BPV2** and (c) **BPV3** with CB[8] in the presence of 0.05 M sodium hydrosulfite at 20 °C. The concentration of conjugated radical cation was 2.5×10^{-5} M in H_2O.

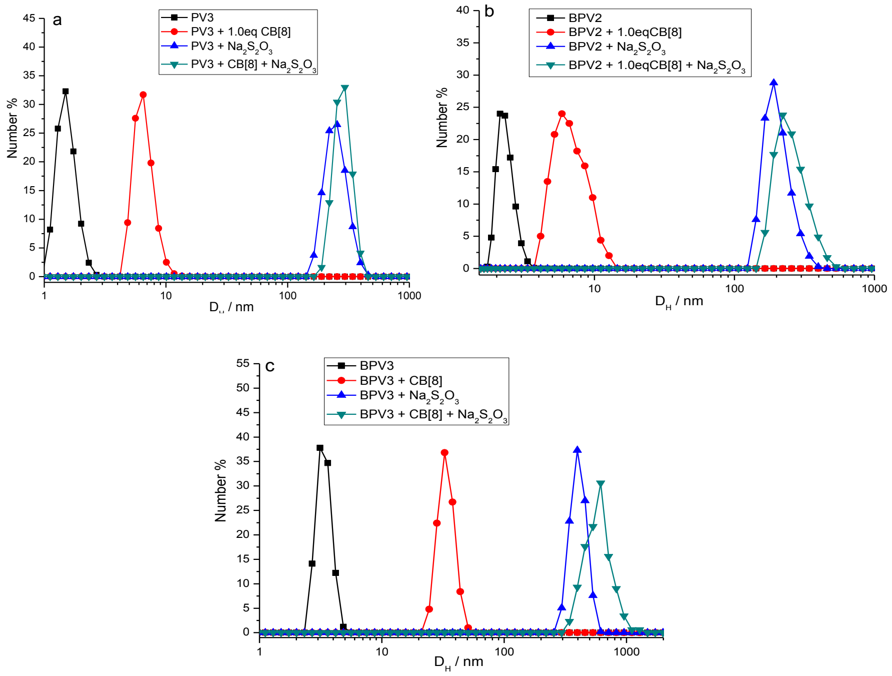

Figure S21. DLS plots of (a) 0.05 mM **PV3**, (0.05 mM **PV3** + 1.0 eq CB[8]), (0.05 mM **PV3** + 0.05 M $Na_2S_2O_3$) and (0.05 mM **PV3** + 1.0 eq CB[8] + 0.05 M $Na_2S_2O_3$) respectively; (b) 0.05 mM **BPV2**, (0.05 mM **BPV2** + 1.0 eq CB[8]), (0.05 mM **BPV2** + 0.05 M $Na_2S_2O_3$) and (0.05 mM **BPV2** + 1.0 eq CB[8] + 0.05 M $Na_2S_2O_3$) respectively and (c) 0.05 mM **BPV3**, (0.05 mM **BPV3** + 1.0 eq CB[8]), (0.05 mM **BPV3** + 0.05 M $Na_2S_2O_3$) and (0.05 mM **BPV3** + 1.0 eq CB[8] + 0.05 M $Na_2S_2O_3$) respectively at 20 °C.

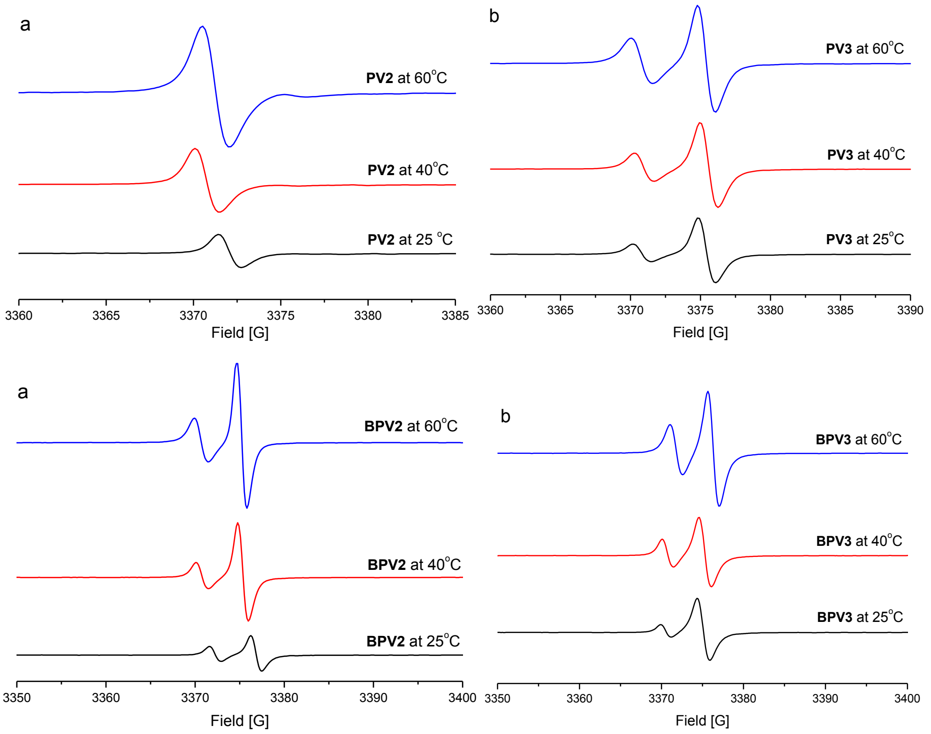

Figure S22. EPR spectra of (a) **PV2**; (b) **PV3;** (c) **BPV2** and (b) **BPV3** at different temperatures in H_2O (pH = 7) with 0.05 M $Na_2S_2O_3$. The concentration was 0.1mM.

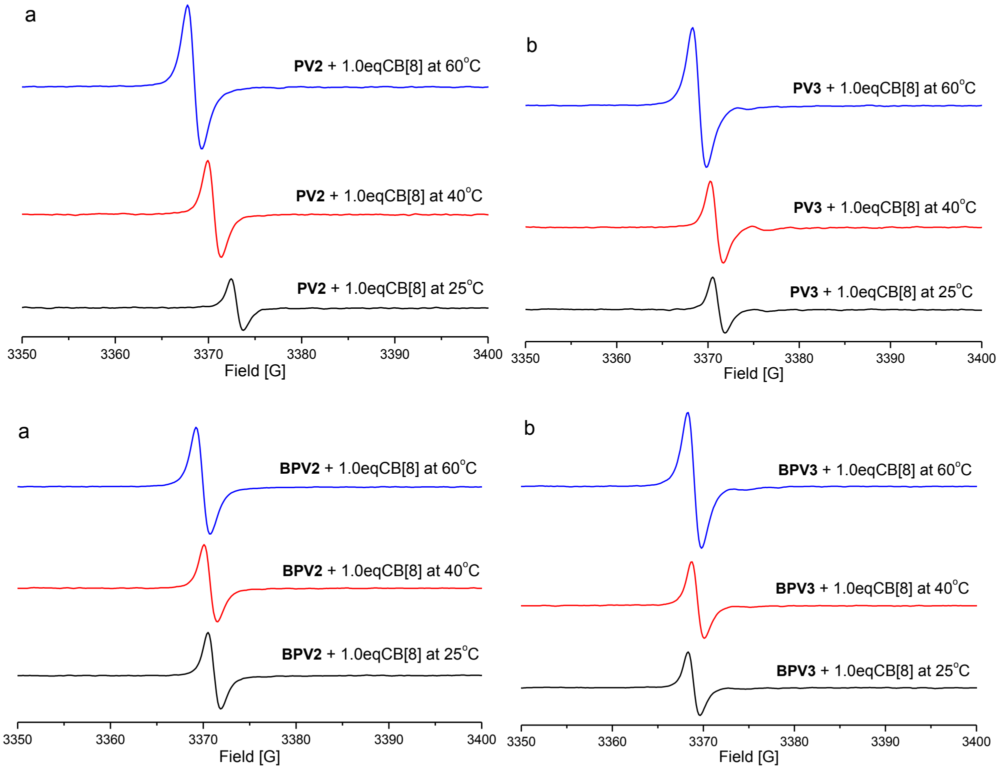

Figure S23. EPR spectra of (a) **PV2 +** 1.0 eq CB[8]; (b) **PV3 +** 1.0 eq CB[8]; (c) **BPV2 +** 1.0 eq CB[8] and (d) **BPV3 +** 1.0 eq CB[8] at different temperatures in H_2O (pH = 7) with 0.05 M $Na_2S_2O_3$. The concentration was 0.1 mM.

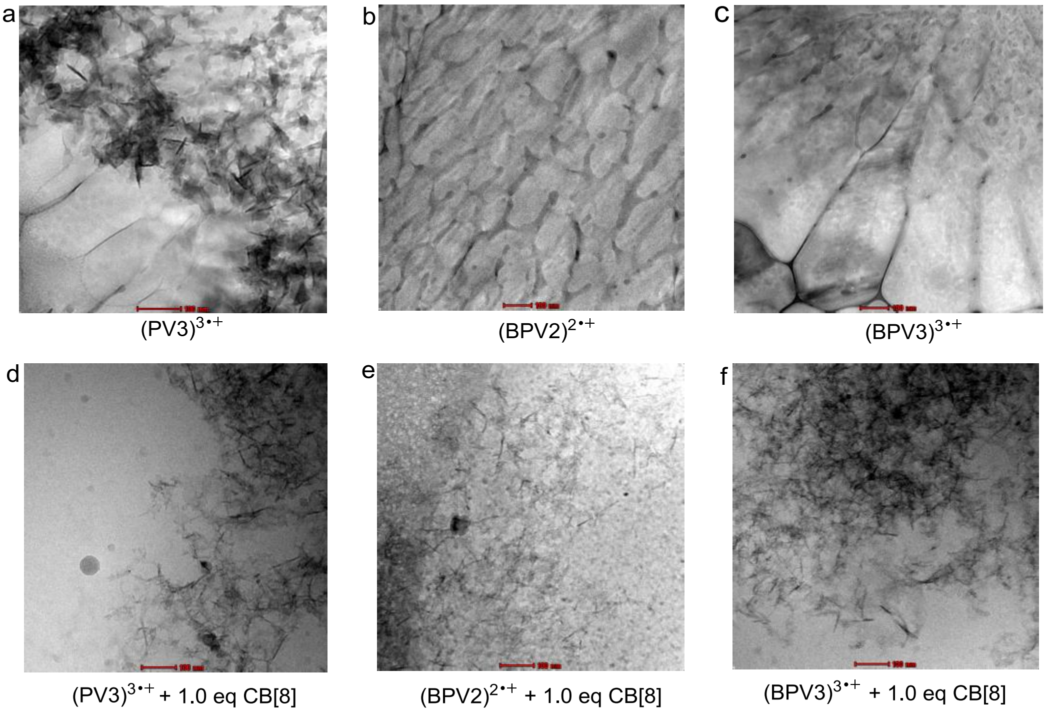

$(PV3)^{3\bullet+}$ $(BPV2)^{2\bullet+}$ $(BPV3)^{3\bullet+}$

$(PV3)^{3\bullet+}$ + 1.0 eq CB[8] $(BPV2)^{2\bullet+}$ + 1.0 eq CB[8] $(BPV3)^{3\bullet+}$ + 1.0 eq CB[8]

Figure S24. Cryo-TEM images of (a) (**PV3**)$^{3\cdot+}$; (b) (**BPV2**)$^{2\cdot+}$; (c) (**BPV3**)$^{3\cdot+}$; (d) (**PV3**)$^{3\cdot+}$ + 1.0 eq CB[8]; (e) (**BPV2**)$^{2\cdot+}$ + 1.0 eq CB[8] and (f) (**BPV3**)$^{3\cdot+}$ + 1.0 eq CB[8]. The concentration was 0.025 mM and the scale bar was 100 nm.

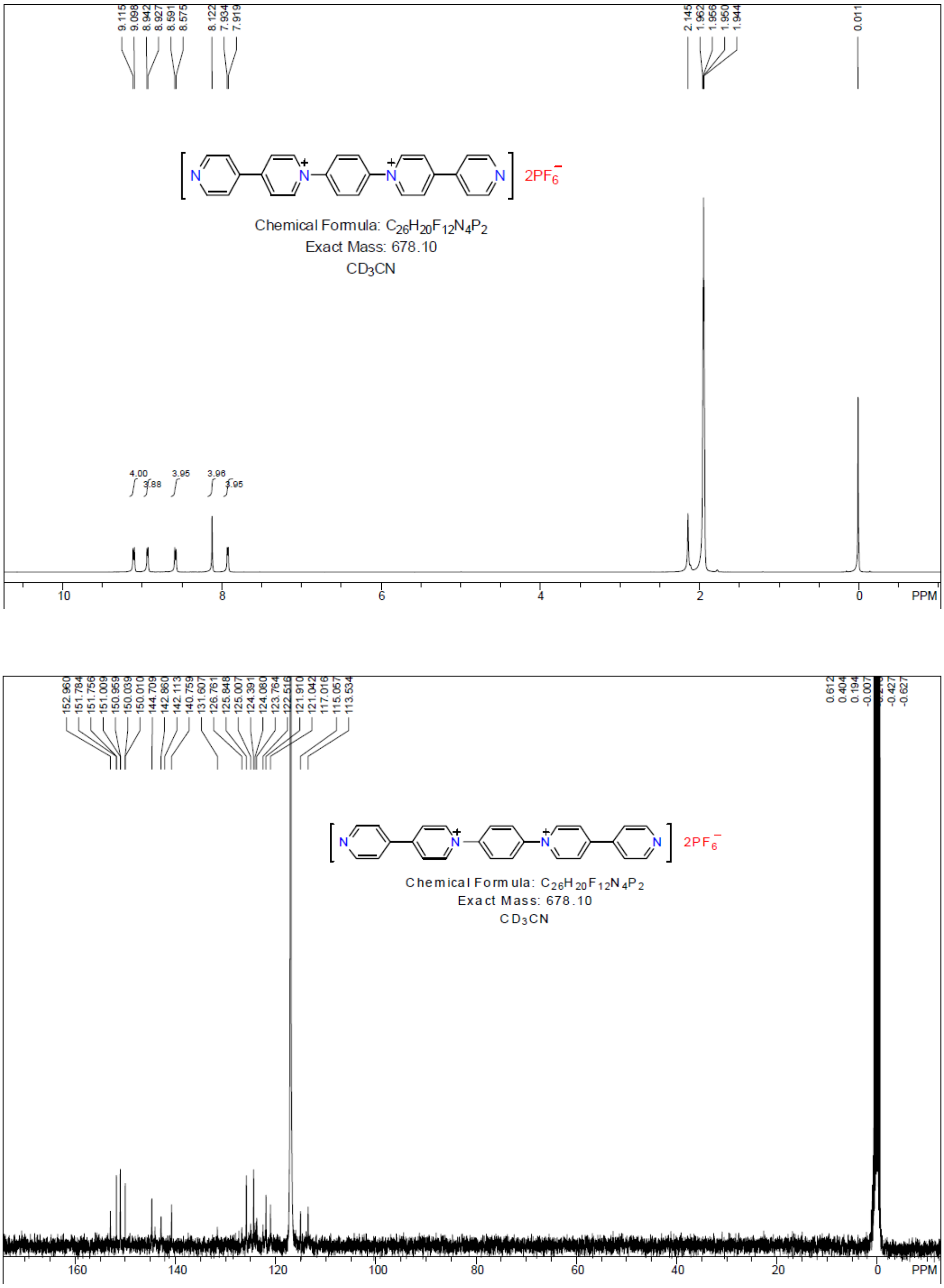

Figure S25. ^{1}H NMR (400 MHz, CD_3CN) and ^{13}C NMR (125 MHz, CD_3CN) spectra of compound **3**.

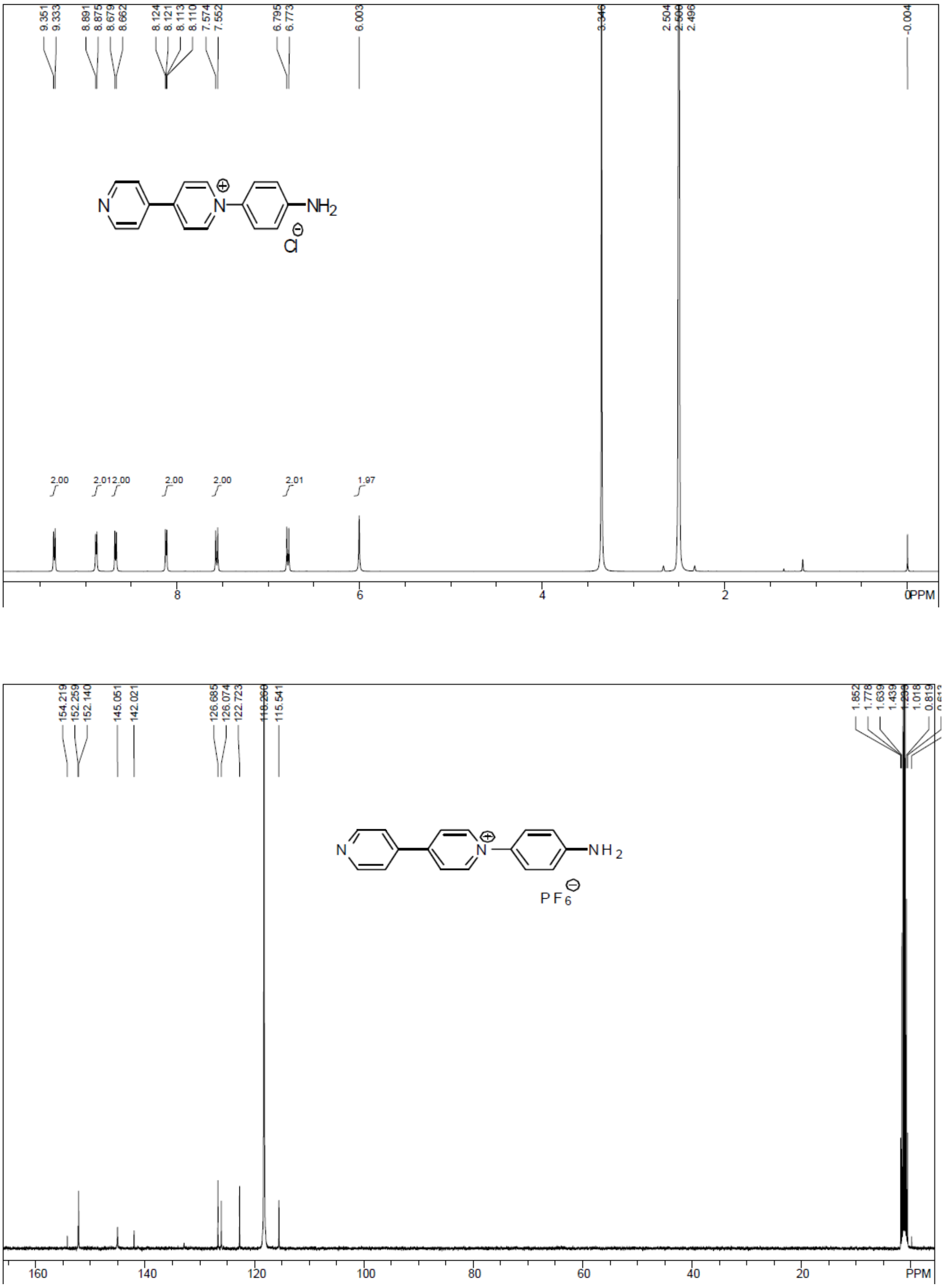

Figure S26. ^{1}H NMR (400 MHz, DMSO-d_6) and ^{13}C NMR (125 MHz, CD_3CN) spectra of compound **4** at 25 ^{o}C.

.

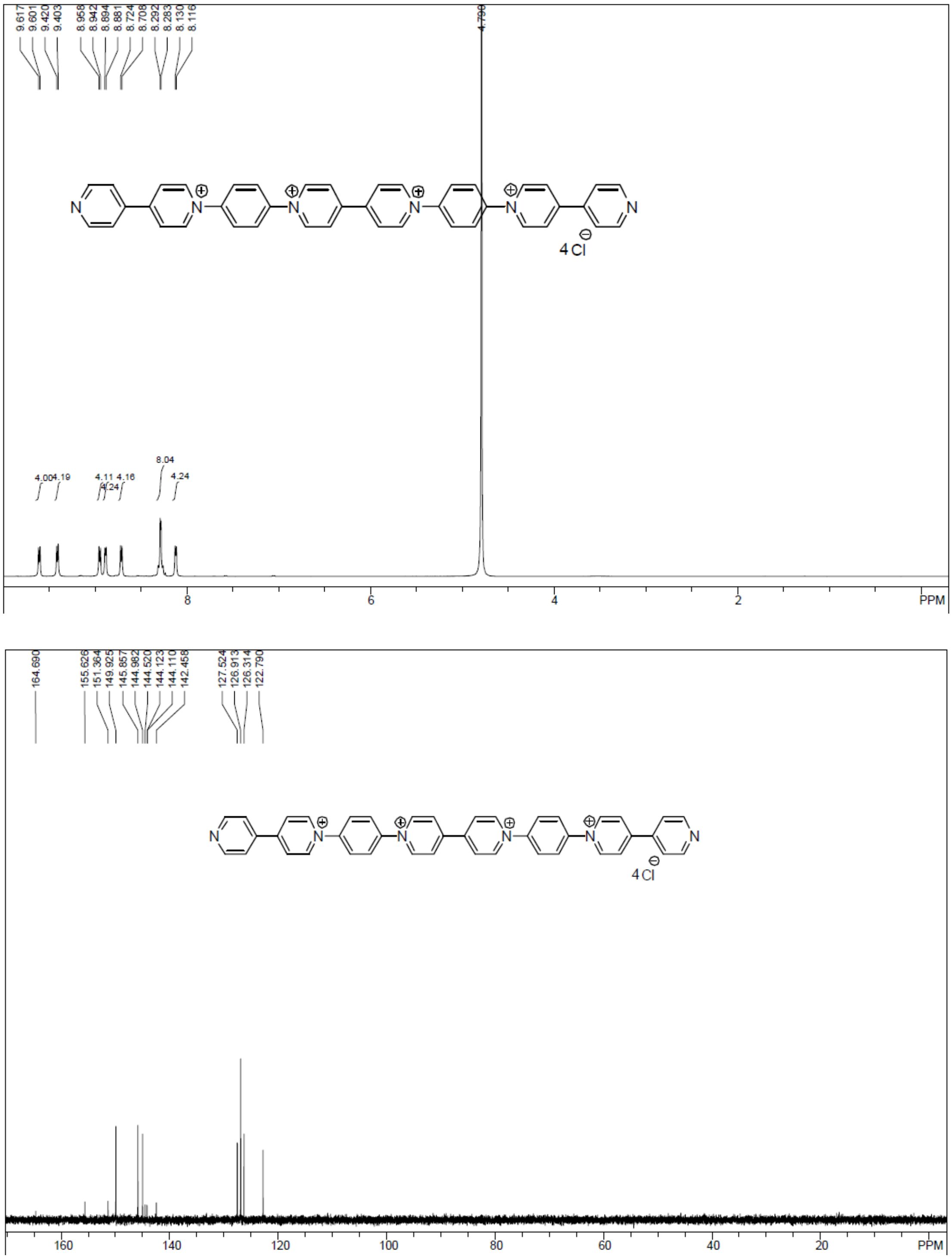

Figure S27. ^{1}H NMR (400 MHz, D_2O) and ^{13}C NMR (125 MHz, D_2O) spectra of compound **5** at 25 ^{o}C.

.

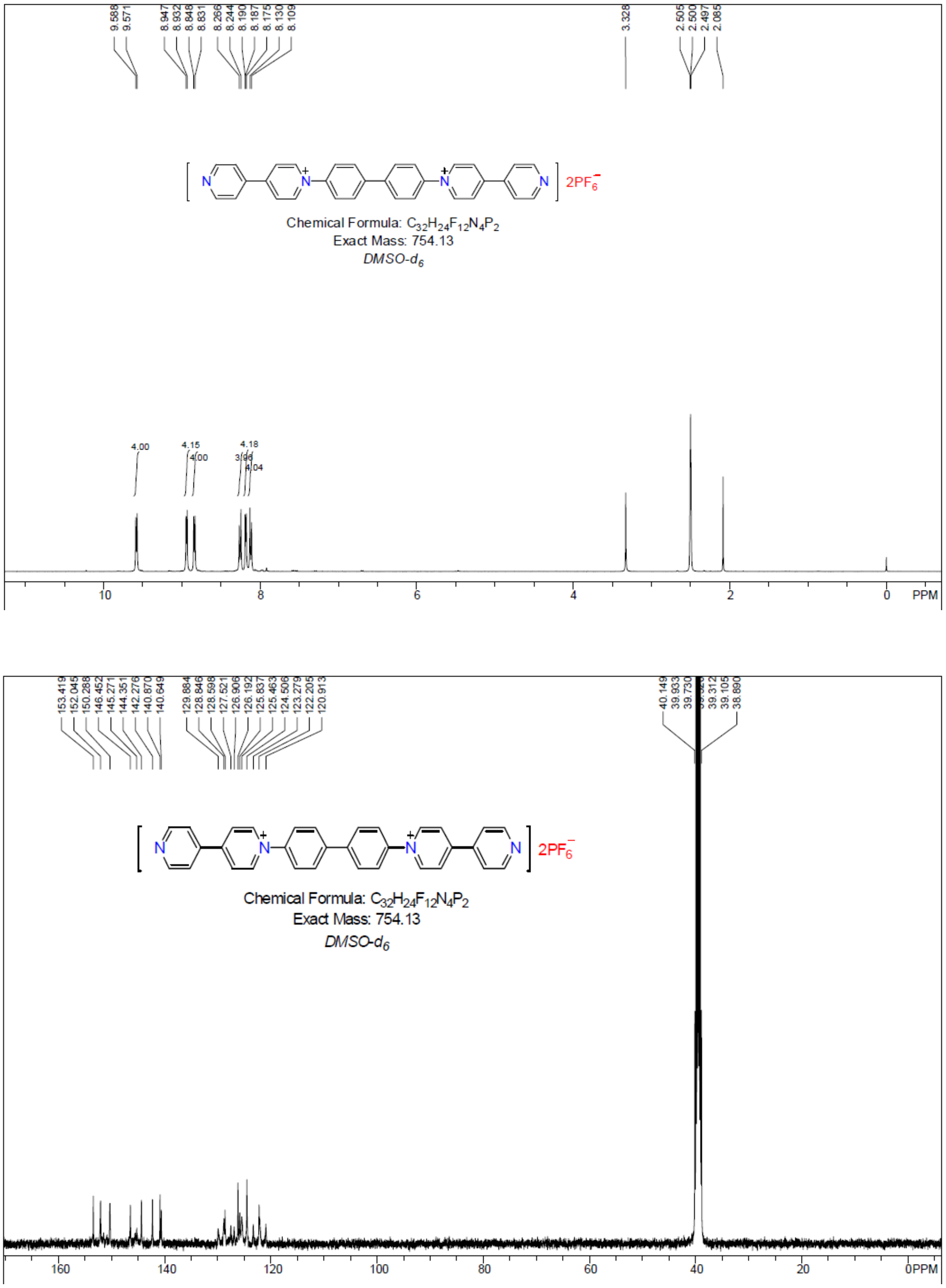

Figure S28. ^{1}H NMR (400 MHz, DMSO-d_6) and ^{13}C NMR (125 MHz, DMSO-d_6) spectra of compound **6** at 25 °C.

.

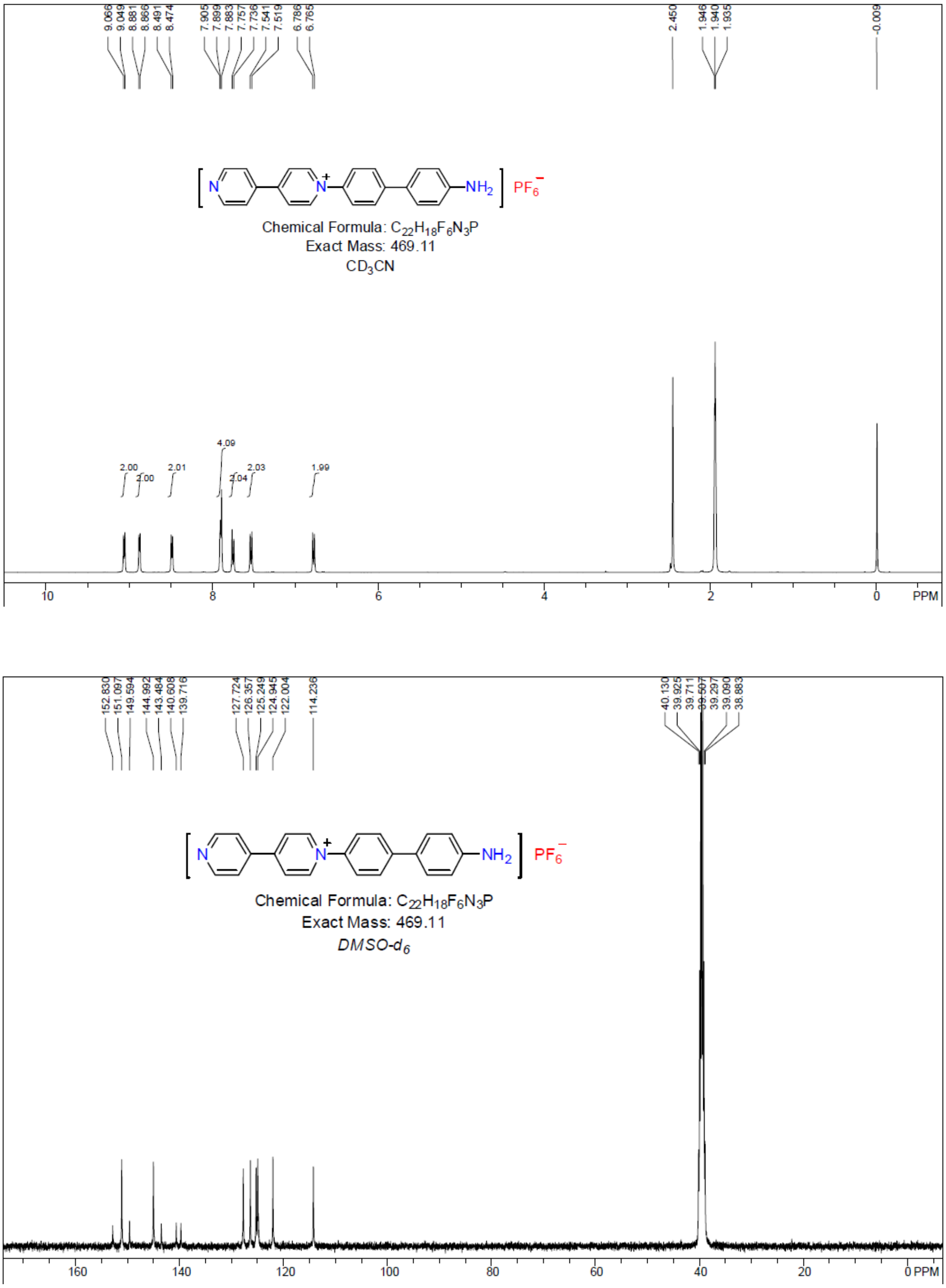

Figure S29. ^{1}H NMR (400 MHz, CD_3CN) and ^{13}C NMR (125 MHz, DMSO-d_6) spectra of compound **7** at 25 °C.

.

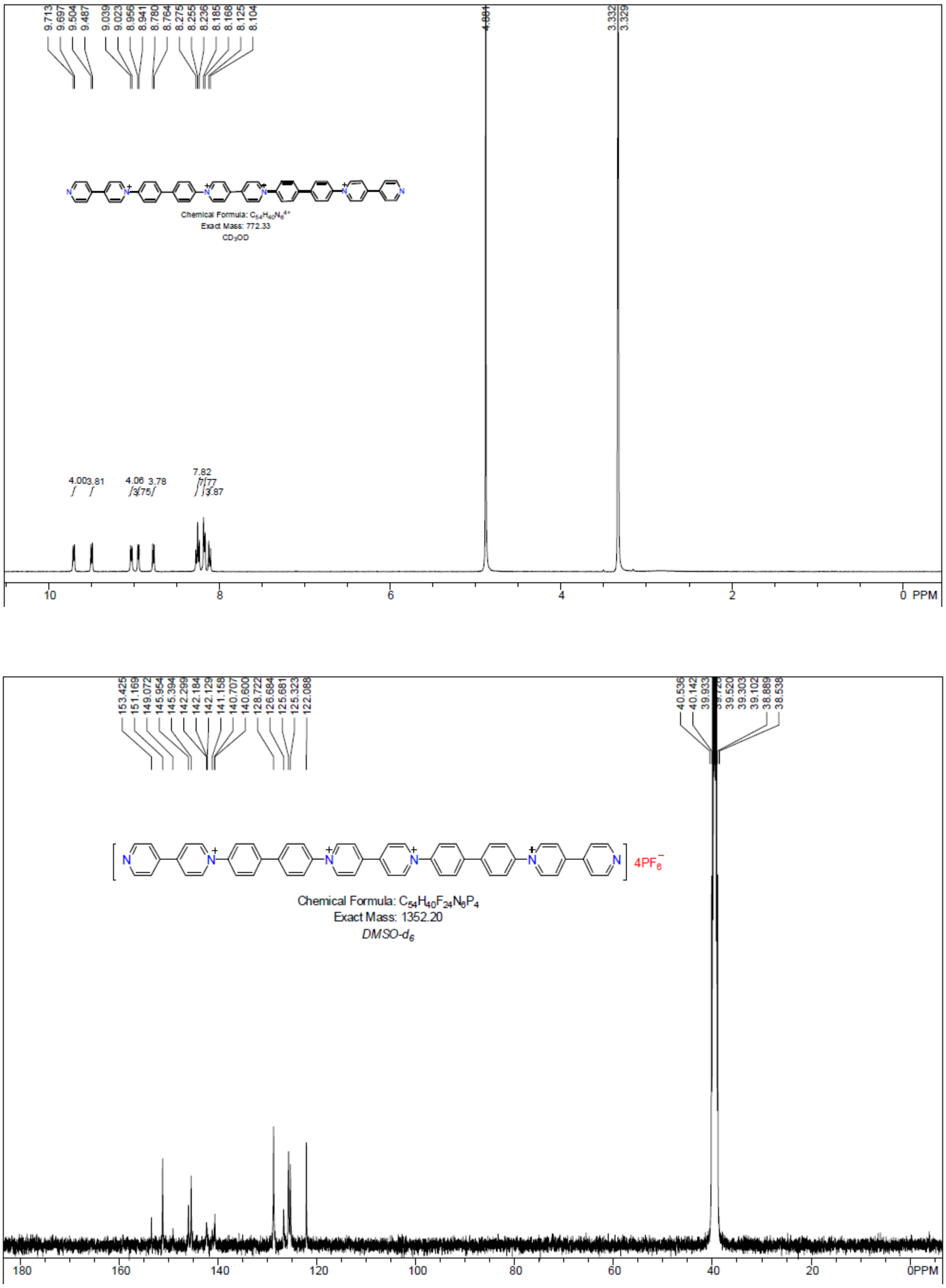

Figure S30. ^{1}H NMR (400 MHz, CD$_3$OD) and ^{13}C NMR (125 MHz, DMSO-d_6) spectra of compound **8** at 25 ^{o}C.

.

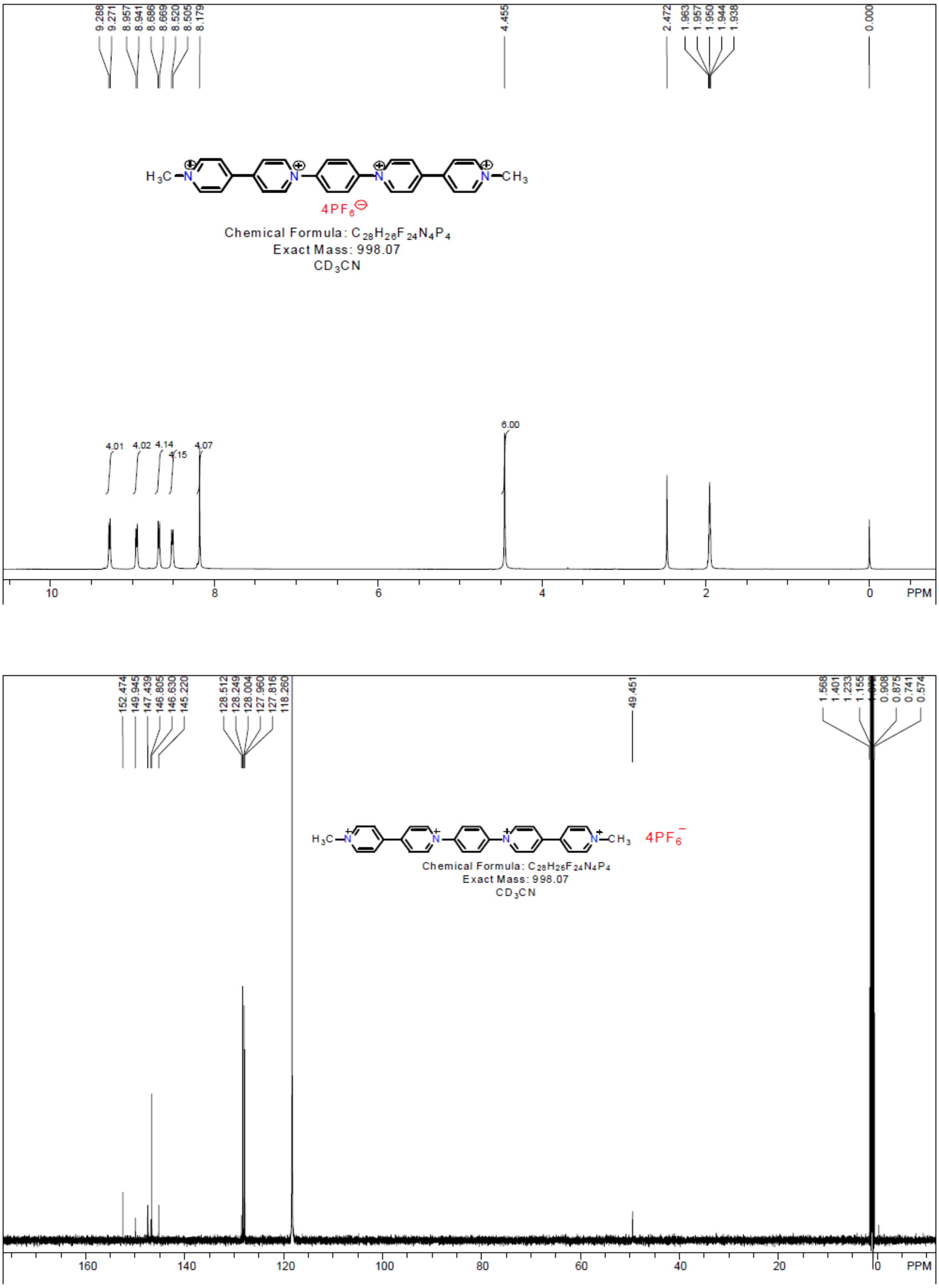

Figure S31. ^{1}H NMR (400 MHz, CD_3CN) and ^{13}C NMR (125 MHz, CD_3CN) spectra of **PV2** at 25 °C.

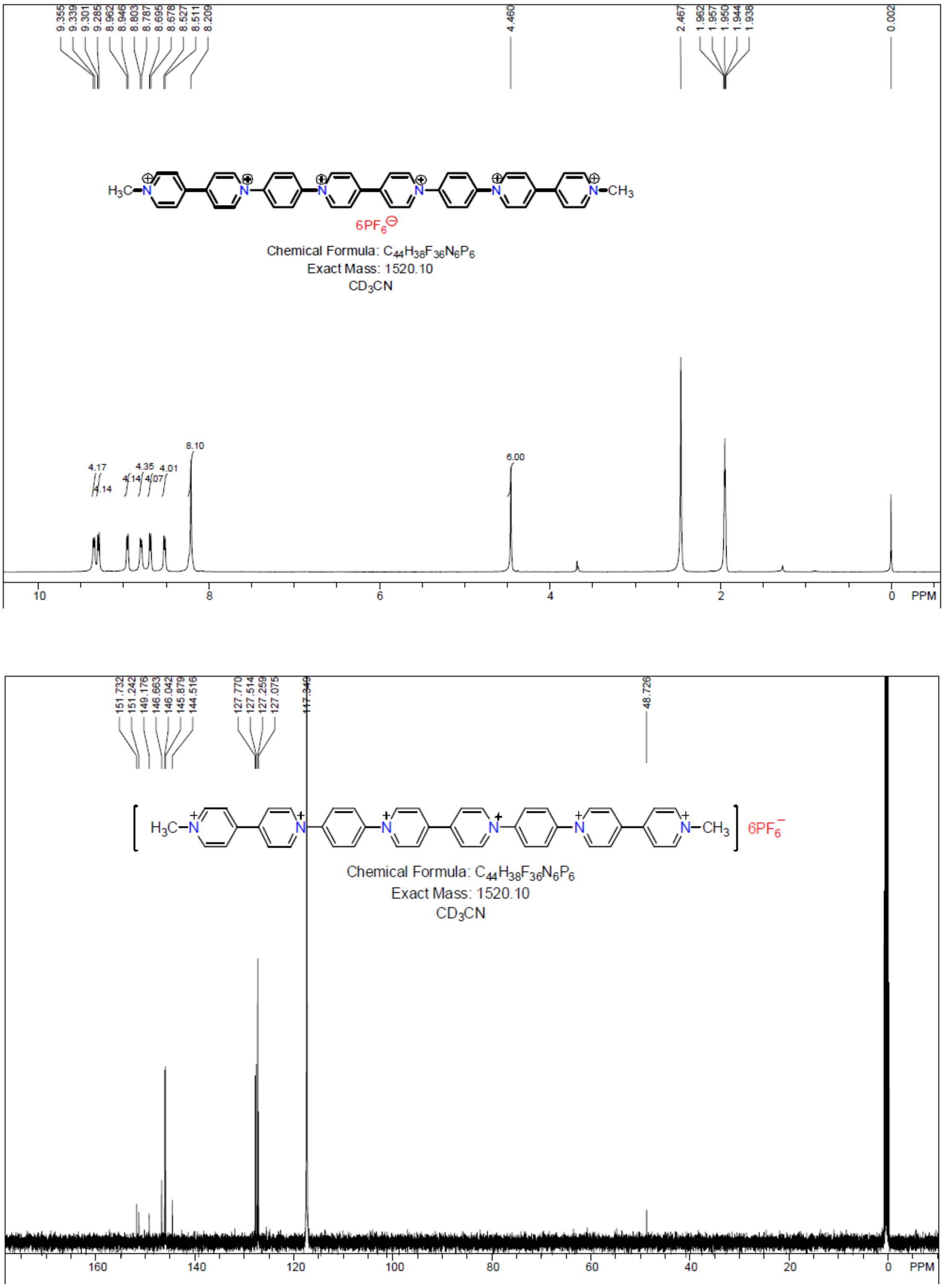

Figure S32. ^{1}H NMR (400 MHz, CD_3CN) and ^{13}C NMR (125 MHz, CD_3CN) spectra of **PV3** at 25 °C.

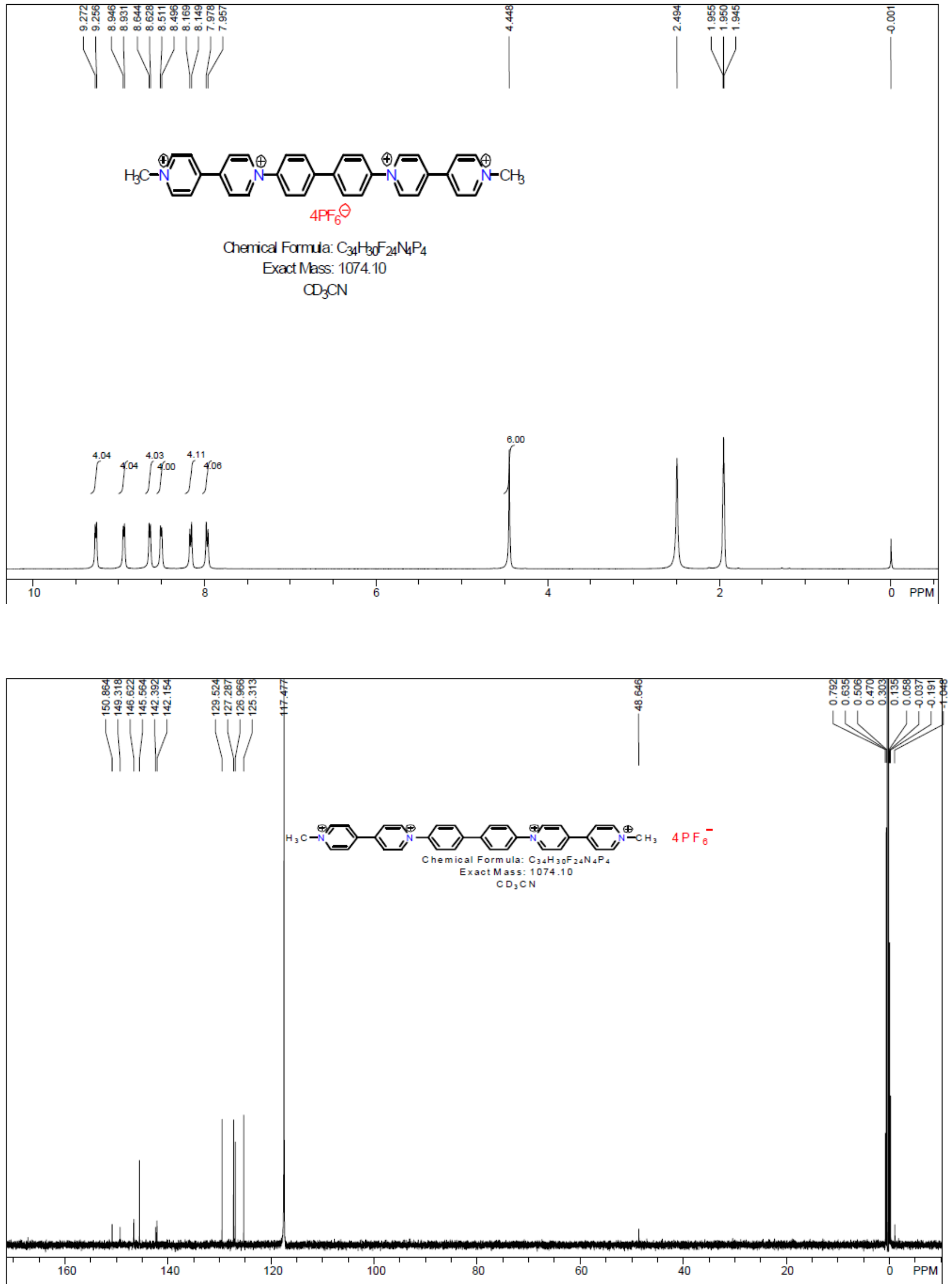

Figure S33. ^{1}H NMR (400 MHz, CD_3CN) and ^{13}C NMR (125 MHz, CD_3CN) spectra of **BPV2** at 25 °C.

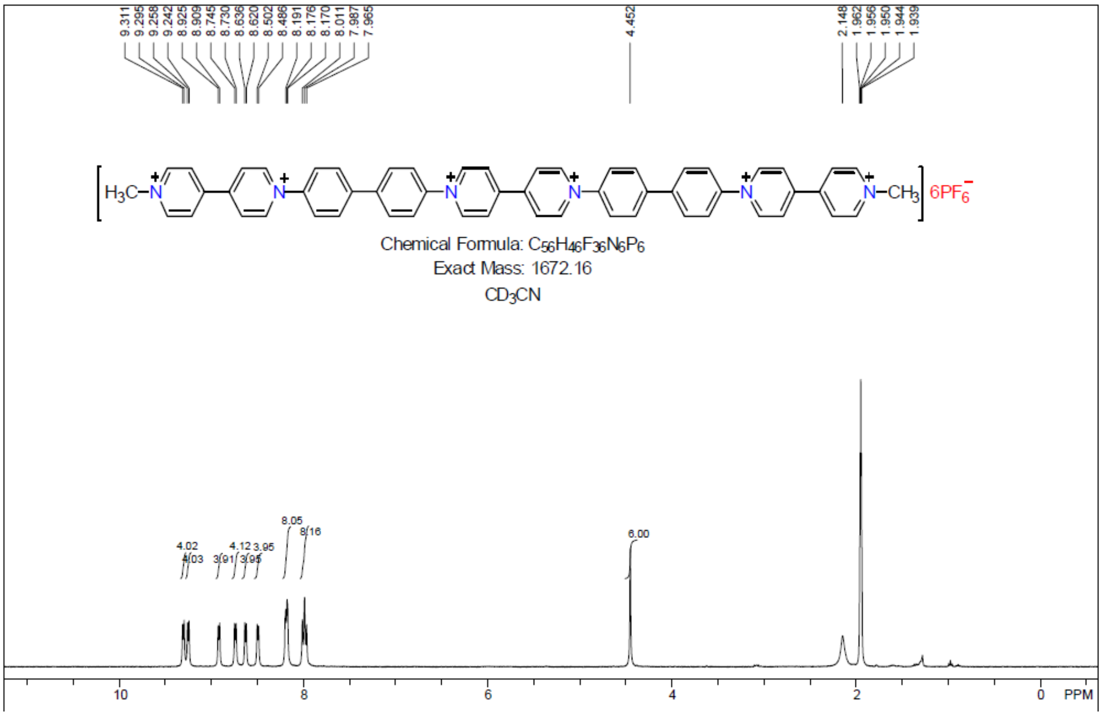

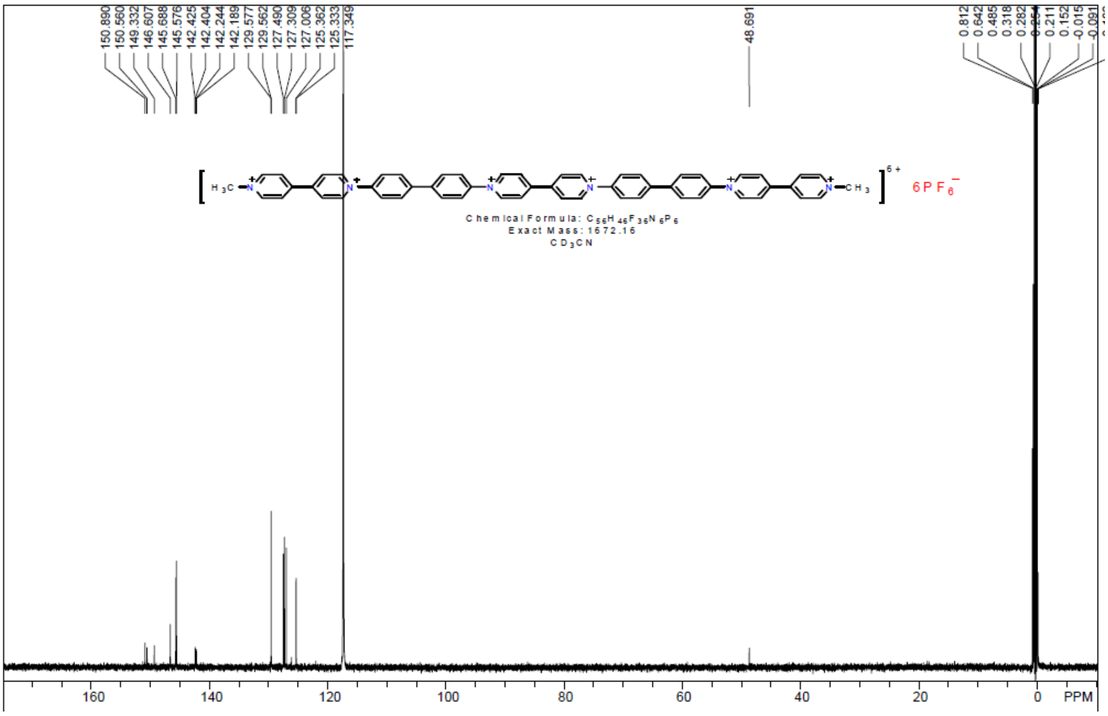

Figure S34. ^{1}H NMR (400 MHz, CD_3CN) and ^{13}C NMR (125 MHz, CD_3CN) spectra of **BPV3** at 25 °C.

References

(1) F. Lin, T.-G. Zhan, T.-Y. Zhou, K.-D. Zhang, G.-Y. Li, J. Wu and X. Zhao, *Chem. Commun.*, 2014, **50**, 7982.

(2) C. Lee, M. S. Moon and J. W. Park, *J. Incl. Phenom. Mol. Recognit. Chemi.*, 1996, **26**, 219.

(3) W. S. Jeon, H.-J. Kim, C. Lee and K. Kim, *Chem. Commun.*, 2002, 1828.